Research on Engineering Structures & Materials
www.jresm.org

Research Article

Influence of calcium sources on strength and self-healing characteristics of bacterial concrete

Gouthami Patnaik Palter [*,1,a], Kanaka Durga Sambhana [1,b], Venkata Giridhar Poosarla [2,c], Potharaju Malasani [3,d]

[1]*Department of Civil Engineering, GITAM School of Technology, GITAM (Deemed to be University), Visakhapatnam, Andhra Pradesh, 530045, India*
[2]*Department of Life Sciences, GITAM School of Science, GITAM (Deemed to be University), Visakhapatnam, Andhra Pradesh, 530045, India*
[3]*Registrar, Apollo University, Chittoor, Andhra Pradesh, 517127, India*

Article Info

Article History:

Received 25 May 2025
Accepted 23 July 2025

Keywords:

Bio-mineralization;
Microbially induced calcium carbonate precipitation;
Calcium precursors;
Strength properties;
Microstructure analysis;
Induced pre-crack width healing

Abstract

Concrete cracking poses significant challenges for infrastructure longevity, leading to costly maintenance and structural weaknesses. This research investigates a sustainable solution using Microbially Induced Calcium Carbonate Precipitation (MICP) with *Bacillus subtilis*, a non-ureolytic bacterial agent, for autonomous crack repair. Alongside M20 grade concrete samples, bacterial concrete specimens were prepared in this study by incorporating three calcium-based precursors-calcium lactate, calcium nitrate, and calcium formate at varying dosages (1%, 2%, and 3% by weight of cement). These precursors stimulate the calcite formation during bio-calcification. Strength performance and self-healing behavior of induced pre-crack widths were evaluated over 91 days, with durability assessments including water absorption, porosity (28 days), and drying shrinkage over 91 days. Results showed that adding calcium precursors did not adversely affect strength. Notably, bacterial concrete with 1% calcium formate showed 31.1% strength increase, while 1% calcium lactate and 2% calcium nitrate achieved 18% and 28% improvements respectively, compared to conventional concrete specimens at 91 days. Samples with 3% calcium formate dosage achieved the lowest porosity (6.1%), which corresponded to the maximum compressive strength of 62MPa through effective pore filling. Remarkably, 1% calcium formate completely healed 2mm crack width by day 91. Scanning Electron Microscopy (SEM), Energy-Dispersive X-ray Spectroscopy (EDS), Fourier Transform Infrared spectroscopy (FTIR), and X-ray diffraction (XRD) analyses confirmed enhanced calcite precipitation and microstructural densification in optimal specimens, particularly with calcium formate. Non-ureolytic microbial systems enhance both strength and crack healing abilities establishing calcium formate at 1% dosage as the optimal precursor, providing a promising, resilient, self-sustaining construction material.

1. Introduction

Despite its ubiquity and seeming simplicity, concrete's intrinsically diverse microstructure results in extremely complex mechanical behavior. At the core of this complexity are the development and spread of micro-crack networks, which are the primary causes of concrete structures' deterioration in strength [1]. Figuring out the impact of cracks reduces the need for expensive repairs and replacements while maximizing the use of concrete. Inadequate understanding and treatment of

*Corresponding author: 1260216403@gitam.in
[a]orcid.org/0000-0002-9491-2048; [b]orcid.org/0000-0002-4756-4191; [c]orcid.org/0000-0001-9827-6336; [d]orcid.org/0000-0001-6336-2103
DOI: http://dx.doi.org/10.17515/resm2025-926ma0525rs

cracks can jeopardize structural integrity and perhaps result in catastrophic failures. Investigations into the mechanisms of fracture propagation yield crucial information for early warning systems and safety assessment procedures. Through improved crack management, concrete service life can be extended to 100 years, which directly supports sustainability objectives by lowering replacement costs and the resulting carbon footprint [2]. In the United States alone, concrete infrastructure upkeep and repair currently cost more than $100 billion a year, with comparable proportionate expenses seen throughout the world. Treatments to remediate the crack using certain traditional methods were employed in the presence of human intervention, which requires incessant periodic investigation and application of external agents such as injecting, pasting techniques, and coatings on the concrete surfaces. However, these traditional remediation methods are limited because of the material's weak heat resistance, moisture sensitivity, labour-intensive and differential coefficient of thermal expansion [3-6]. The manufacture of cement, which is essential for these repairs, accounts for around 7% of carbon dioxide emissions worldwide. Compared to conventional manufacturing methods, bio-cementation reduces carbon emissions by 18–49.6% [7]. Moreover, chemical-based repair products frequently have compatibility problems and present health dangers, which makes maintenance tasks much more difficult [8, 9]. A revolutionary approach to infrastructure resilience is the self-healing concrete paradigm, in which the material is designed to utilize either of the two self-healing mechanisms, one being autonomous crack healing and the other being autogenous crack healing [10-12]. The autogenous healing technique is an organic process, and its healing capacity is possible when there is an addition of high binding mixtures and a delayed hydration process, confining to small cracks closure, i.e., 0.15-0.2 mm is achievable. Although its efficiency can be enhanced with additives like fibres, supplementary cementitious materials (SCMs), and curing agents, it is still inadequate for addressing larger cracks [13, 14]. An autonomous healing mechanism was explicated in order to combat the aforementioned problems by introducing certain intrinsic and extrinsic self-healing materials or agents into the concrete, which remain dormant lest activated by crack formation [15-20]. Cracks being healed with the aid of micro-organisms underlines the intrinsic treatment which relies on a novel technology of “Bio-mineralization” [21, 22], and other methods by incorporating polymers, carriers categorize extrinsic treatment which are of high cost [1, 23-26]. A promising subset of autonomous healing mechanisms involves the microbially induced calcium carbonate precipitation (MICP) technique for addressing the micro-crack networks in concrete structures. This innovative bio-chemical process converts organic substrates into inorganic compounds through the catalysis of bacteria, creating an alkaline environment that leads to calcium carbonate precipitation [27]. Calcium lactate, calcium nitrate, calcium formate, calcium acetate, calcium chloride, and calcium glutamate are such compounds that are supplemented as calcium precursors for undergoing the MICP process in self-healing concrete, either through metabolic conversion of organic compounds or ureolysis, or denitrification precipitation mechanism [21, 28-32]. Amongst which calcium lactate, calcium nitrate, and calcium formate are applicable at the field-scale level for the enhancement of concrete properties [33]. Calcium lactate is bio-compatible, low-cost, easily accessible, and can be directly added into the concrete matrix in mixing water [34-36]. Calcium nitrate is globally used in the admixture/agriculture industry scale. It acts as an accelerator; inhibits corrosion, is compatible with other additives, and is cost-effective [30, 37, 38]. Calcium formate is used in multiple roles in varied field-scale applications, especially in cement-based industries. It acts as an accelerator, anti-freezing agent, and is cost-effective [39, 40]. Calcium acetate and calcium chloride are also cost-effective, but calcium chloride alone may not be considered the optimal choice in MICP studies [41]. A study reported that MICP treatment exhibited a lifecycle cost decrease of roughly 98% when compared to conventional treatment approaches [7, 40, 41]. Most MICP studies have centered on ureolytic bacteria such as *Sporosarcina pasteuriia* and *Bacillus subtilis* species, which catalyze urea hydrolysis to produce carbonate ions. However, ureolytic pathways can result in ammonia by-products and are sensitive to pH and substrate conditions, limiting their scalability. Non-ureolytic bacteria like *B. subtilis* offer a biologically safer and chemically stable alternative, yet remain underexplored in MICP-based self-healing concrete. A study reported that recovery of compressive strength of the specimens was about 80% due to the MICP mechanism [42-44]. Certain study findings revealed a 32% enhancement in compressive strength and a 37% enhancement in flexural strength attributed to the deposition of ($CaCO_3$),

which filled micro voids and densified the concrete [42, 45-50]. Previous research demonstrated that MICP-treated concrete exhibited a 70% reduction in water permeability compared to untreated samples. The addition of calcium lactate alone directly would increase the strength in the concrete when used at up to 1 and 2% and potentially up to 3% by mass of cement [51]. The influence of the three self-healing agent's calcium lactate, calcium nitrate, and calcium formate on setting time, hydration kinetics, rheology, and compressive strength in the presence of spore-forming bacterial species was studied in the cement mortar. However, the ability of these self-healing agents in terms of strength and crack healing was not assessed, particularly in the context of non-ureolytic microbial systems [52]. This study addresses this gap by systematically evaluating the influence of three calcium precursors, i.e., calcium lactate, calcium nitrate, and calcium formate, on the mechanical properties and crack healing performance of *B. subtilis*-based microbial concrete. The precursors were incorporated at three dosage levels (1, 2, and 3 % by weight of cement (bwc)), and performance metrics included mechanical strength, porosity, water absorption, drying shrinkage, self-healing performance, and microstructural characterization.

2. Materials and Methods

2.1. Cement and Calcium Sources

The Ordinary Portland Cement (OPC) of 53 grade, complying with IS 12269: 2013, was used in this study. Potable water was utilized that complied with IS 456: 2000. The precursors incorporated in the study are Calcium lactate ($CaC_6H_{10}O_6.5H_2O$), (L), LR grade was from Triveni Interchem Pvt. Ltd., Gujarat; Calcium nitrate ($(CaNO_3)_2.4H_2O$), (N), LR grade was from locally made United Scientific Chemicals Pvt ltd., Visakhapatnam; Calcium formate ($Ca(HCOO)_2$),(F), 99% LR grade was from Future Lab, Bangalore. The physical properties of the cement, fine and coarse aggregates, including fineness of cement (R), specific gravity (G_s), water absorption (W_a), fineness modulus (FM), standard consistency (P), initial and final setting time according to the IS codes were tabulated in Table 1. The methodology adopted in this study is illustrated (Fig. 1).

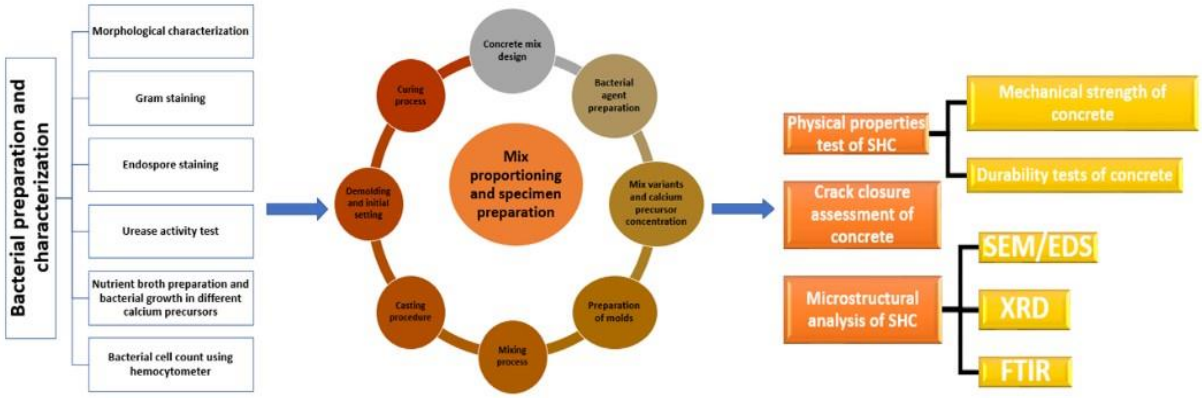

Fig. 1. Schematic flowchart of the methodology employed in the present study

Table 1. Physical properties of cement and aggregates

S.No	Materials	R	G_s	W_a	FM	P	Shape	Initial and Final setting time (min)	Referral codes
1	Cement	2.3%	3.1	-	-	33%	-	85 and 381	IS 4031 Part1:1996 IS 4031 Part4:1988 IS 4031 Part5:1988
2	Fine	-	2.6	0.5	2.2	-	-	-	IS 2386 Part1:1963 IS 383:2016
3	Coarse	-	2.7	0.55	6.0	-	Angular	-	

2.2 Bacterial Medium Preparation

In this study, *B. subtilis* was procured in the lyophilized form from Proprenz Biotech Pvt. Ltd., located in Hyderabad. The bacterium procured had undergone the microbiological investigations and examination in GITAM University, at Department of Microbiology, Visakhapatnam.

2.2.1 Identification of Bacteria

Nutrient broth (NB) was used for general cultivation of microorganism contains following ingredients: peptone (5 g/L), sodium chloride (5 g/L), HM peptone (1.50 g/L), and yeast extract (1.50 g/L). Utilizing nutritional agar media at pH-11 and 37 °C in an incubator, the bacterial spores were grown in a petri plate. Morphological examination was carried out using the Gram staining method and Endospore staining to determine bacterial structure and characteristics [53, 54]. Under the former method, to make a smear, a sterile inoculating loop was used to take a loopful of bacterial culture and spread it evenly throughout the surface. The smear was left to fully air dry. From a pure 18–24 h culture, the slant was infected with a strong diagonal streaking of the agar surface. For 24 h to 48 h, inoculated tubes were incubated at 35 to 37 °C with their caps unfastened. A microscope equipped with an immersion oil lens was used to study the coloured bacterial cells at a 100X magnification. In the latter method, the *B. subtilis s*pores were tested for their ability to form endospores by Schaeffer–Fulton endospore staining technique.

2.2.2 Urease Test

To identify bacteria capable of hydrolysing urea, the urease test was conducted using the urease enzyme. According to the conventional method, Christensen's urea agar slants were made using the following ingredients (per liter): urea (20.0 g), phenol red indicator (0.012 g), agar (20.0 g), sodium chloride (5.0 g), yeast extract (0.1 g), potassium dihydrogen phosphate (2.0 g), peptone (1.0 g), and dextrose (1.0 g). To avoid pressure build-up, the medium was distributed into test tubes and autoclaved for 15 minutes at 121°C with loose-fitting lids. To produce slanted surfaces, tubes were placed at an oblique angle during cooling after sterilization.

2.2.3 Culturing of the Bacterium

The bacterial strain was grown in commercial nutrient broth (HiMedia Laboratories, India) prepared by dissolving 6.5 g of powder in 1.5 L of distilled water, following the manufacturer's instructions. The exact composition of the broth reflects proprietary formulations including typical components such as peptone, sodium chloride, and yeast extract. Sterile HCl or NaOH was used as needed to bring the pH down to 7.0 ± 0.1.

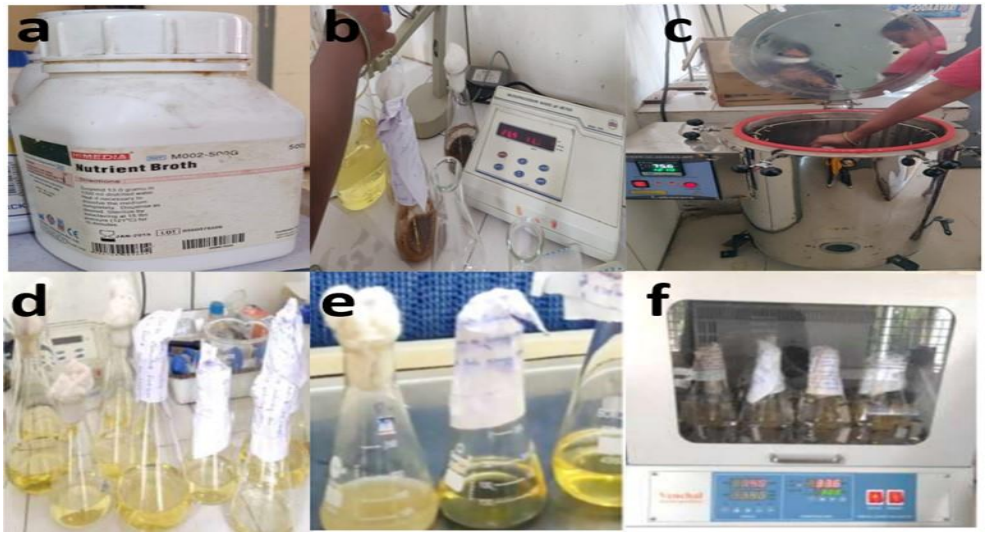

Fig. 2. Steps of media preparation. a. medium, b. pH setting, c. autoclaving at 121 °C for 15 min, d. broths after autoclave, e. inoculation using fresh pre-inoculum, and f. incubation in an orbital shaker for 24 h

To ensure sterility, the medium was poured into the proper containers, covered with aluminum foil and cotton plugs, and autoclaved for 15 minutes at 121 °C. A 2% (w/v) inoculum concentration was attained by aseptically transferring 5 g of bacterial biomass into 250 mL of sterile nutrient broth for inoculum preparation. This prepared inoculum was subsequently used to seed 1.5 L of nutrient broth in each experimental batch. For 24 hours, the infected broth was incubated at 30 °C with agitation at 148 rpm in an orbital shaker to guarantee proper aeration and mixing. The optical density (OD) at 600 nm was measured periodically to track growth, and a turbidity test was conducted to evaluate the impact of each calcium source on bacterial proliferation. The compatibility of the bacteria with different calcium sources, which are essential for the MICP process in self-healing concrete applications, was revealed by these studies. The bacterium medium preparation process is illustrated (Fig. 2).

2.2.4 Bacterial Cell Count Using Hemocytometer

Following a 24-hour incubation period, 0.1 µL of the bacterial culture was added to 1000 µL of diluent using a sterile pipette. This solution was serially diluted by a factor of 10 to achieve an appropriate dilution, with 10^{-1} identified as optimal. A cleaned hemocytometer featuring a grid with a volume of 0.1 mm^3 divided into five square blocks was filled with the diluted solution (Fig. 3). The spore count was observed under a microscope at 40X magnification, yielding a total count of live cells. Based on this data, the bacterial cell concentration was calculated using Eq. (1), and Eq. (2).

$$Average\ number\ of\ \ cells = \frac{Average\ of\ live\ cells}{Number\ of\ square\ blocks} \quad (1)$$

$$Bacterial\ cell\ concentration = Dilution\ factor\ X\ Average\ number\ of\ cells\ X\ 10^{-4} \quad (2)$$

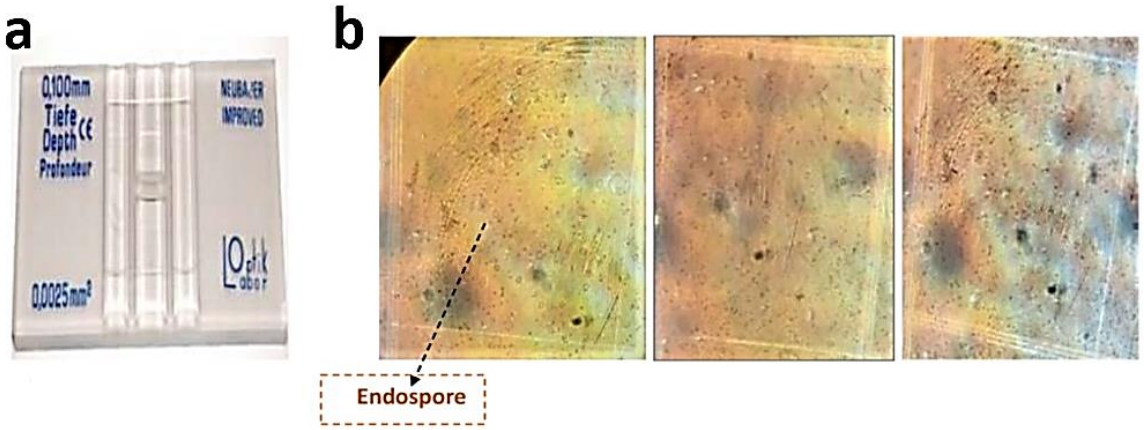

Fig. 3. Hemocytometer and b. square grids of hemocytometer

2.3 Concrete Mix Proportions

IS 10262:2019 was used to carry out the concrete mix design for M20 grade. This study compares the effects of nutrients in bacterial concrete (BC) on the strength and healing qualities of concrete. The conventional concrete (CC) with cement (350 Kg/m^3, fine aggregate 715.97 Kg/m^3, coarse aggregate 1207.84 Kg/m^3, and water 168 Kg/m^3) was designed. Nine different types of bacterial concrete mixes, split into three sets, inclusive of calcium lactate, calcium nitrate, and calcium formate precursors, were fabricated as shown in Table 2. Set A denoted bacterial specimens embedded with the required bacterial medium by incorporating: 1% dosage of calcium lactate as (1BC-L), 2% dosage of calcium lactate as (2BC-L), and 3% dosage of calcium lactate as (3BC-L). Set B denoted bacterial specimens embedded with the required bacterial medium by incorporating:

1% dosage of calcium nitrate as (1BC-N), 2% dosage of calcium nitrate as (2BC-N), and 3% dosage of calcium nitrate as (3BC-N). Set C denoted bacterial specimens embedded with the required bacterial medium by incorporating: 1% dosage of calcium formate as (1BC-F), 2% dosage of calcium formate as (2BC-F), and 3% dosage of calcium formate as (3BC-F).

Table 2. Mix proportions and dosages

Type of mix		Required bacterial medium (cells/mL)	Calcium lactate (bwc)	Calcium nitrate (bwc)	Calcium formate (bwc)
CC		-	-	-	-
1BC-L	Set A	10^5	1%	-	-
2BC-L		10^5	2%	-	-
3BC-L		10^5	3%	-	-
1BC-N	Set B	10^5	-	1%	-
2BC-N		10^5	-	2%	-
3BC-N		10^5	-	3%	-
1BC-F	Set C	10^5	-	-	1%
2BC-F		10^5	-	-	2%
3BC-F		10^5	-	-	3%

2.4 Concrete Specimen Preparation, Casting, and Curing

In the current investigation study, the concrete specimens were cast according to the specifications as per IS 516:1959, and outlined the protocols for preparation, casting, and curing of the concrete samples [55]. To thoroughly evaluate the mechanical performance and self-healing properties of the bacterial concrete, several specimen geometries were created. These included prismatic specimens with dimensions of (100 × 100 × 500 mm), cylindrical specimens with dimensions of (150 × 300 mm), and cubic specimens with dimensions of (100 × 100 × 100 mm). The concrete mixture was formulated in compliance with IS 10262:2019, the bacterial medium (containing *B. subtilis* with a required cell concentration of 10^5 cells/mL), and the calcium-based sources. The bacterial medium and calcium precursors were added directly to the mixing water to ensure even dispersion throughout the concrete matrix. The volume of the bacterial medium required for each specimen type was determined using the Eq. (3)[56] for the preparation of bacterial concrete, wherein the expression in the denominator represents the concentration of the prepared bacterial inoculum, experimentally estimated based on OD600 measurements and a standard calibration curve for *B. subtilis*. The casting process of the conventional and bacterial specimens is embellished (Fig. 4a) and (Fig. 4b).

$$Bacterial\ medium\ volume\ (mL) = \frac{Water\ (L) \times 1000\ \times 10^5}{Bacterial\ cell\ concentration\ (cells/mL)} \quad (3)$$

For 24 hours, the concrete examples were first set at room temperature, which was roughly 27 ± 2 °C. The specimens were carefully removed from their molds using techniques intended to avoid structural damage after the initial setting step was finished. Bacterial concrete specimens were demoulded with extra caution to maintain the integrated bacterial cells' survival and activity during the removal procedure. After demoulding, as per the guidelines, the specimens were immersed in a curing tank filled with potable water maintained at a constant temperature of 27 ± 2 °C. For bacterial concrete, the bacterial medium and calcium-based precursors were expected to react within the matrix during curing, facilitating self-healing mechanisms and enhancing the strength properties of the concrete.

(a)

Fig. 4a. Casting of traditional concrete specimens- cubes, beams, cylinders

(b)

Fig. 4. (a) Casting of traditional concrete specimens- cubes, beams, cylinders and (b) Casting of bacterial concrete specimens- cubes, beams, cylinders

2.5 Mechanical Strength Properties

The mechanical strength properties test includes flexural, split tensile, and compressive strength, performed according to IS 516 (Part 1): 2021 [57-59]. These were performed on the conventional concrete and three sets of bacterial concrete mixes for an age period of 3, 7, 14, 21, 28, 56, and 91 days. At the stipulated curing periods, specimens were removed from the curing tank, and any surface water was wiped off using a clean, dry cloth to ensure accurate measurements. The compressive strength test was performed on the cubical specimens by removing them from the curing tank at a specified age period and testing under a compressive testing machine (CTM)[57]. The load is applied at a controlled rate of 14 N/mm^2/min until the specimen can no longer sustain any additional load. The compressive strength (Fc) was calculated using the Eq. (4). Three-point bending test was conducted on prismatic specimens wherein the specimens were laid on the bed of the universal testing machine (UTM) on which two rollers were positioned [59]. The load was applied axially and symmetrically without causing torsional stress or constraints on the specimen. The rate of loading was maintained at 0.7 N/mm^2/min until failure. The failure pattern was analyzed as per the protocols mentioned in the codal provision. The flexural strength (F_b) was determined using the Eq. (5.1) and Eq. (5.2). The split tensile strength test was conducted on cylindrical specimens [58]. Within the CTM, the specimen was positioned horizontally between two loading wooden strips touching the top and bottom of the device. The split tensile strength (Fsp) was determined using an Eq. (6).

$$F_c\ (MPa) = \frac{F}{A_c} \tag{4}$$

Where F is the maximum load applied (in N) and Ac is the area of the specimen (in mm^2)

$$F_b(MPa) = \frac{P \times L}{B \times D^2}\,(For\ a\ failure\ within\ the\ middle\ third\ of\ the\ span) \tag{5.1}$$

$$F_b(MPa) = \frac{3P \times a}{B \times D^2} (For\ a\ failure\ outside\ the\ middle\ third) \quad (5.2)$$

Where P is the maximum load applied (in Newton), L is the effective span length (mm), B is the width (mm), D is the depth (mm), and a is the distance from the support to the failure point (mm).

$$F_{sp} = \frac{2P}{\pi ld} \quad (6)$$

Where P is the maximum load applied to the specimen (in Newton), l is the length of a cylinder (mm), and d is the cross-sectional dimension of the cylindrical specimen (mm).

2.6 Durability Tests of Concrete

2.6.1 Drying Shrinkage

In general, the parameters studied under the classification of durability are physical, chemical, mechanical, and microstructural. The long-term performance of a structure and its service life is mainly influenced by a critical durability parameter, i.e., drying shrinkage, wherein, due to the loss of moisture, there will be a reduction in concrete volume. This phenomenon plays a vital role in evaluating the dimensional stability and crack-resistance of concrete, especially in structures exposed to varying environmental conditions [20, 60]. The drying shrinkage test was conducted as per IS 4031 Part 10: 1988 [61, 62].

Fig. 5. (a) Reference rod and (b) testing specimen

Mortar beam mould specimens of size 25 mm x 25 mm x 285 mm were cast both for the cement paste with and without bacterial medium embedded with calcium sources. After 24 hours, specimens were demoulded and divided into two categories: one was moist, dry, and sun-dry conditions. Moist Drying: These specimens were exposed in a room at a controlled temperature of 27 ± 2 °C. Sun Drying: The specimens in this group were placed in an open environment under direct sunlight, simulating exposure to atmospheric drying. The length comparator apparatus was used to measure the length change in the specimens at regular intervals, (Fig. 5). The reference points on the specimen were aligned with the comparator pins for consistent measurement. The average difference in length of three specimens was the nearest 0.05 % of the effective gauge length, and this difference was reported as drying shrinkage (%) using Eq. (7).

$$\text{Drying shrinkage } (\%) = \frac{\Delta L}{L_0} \text{x } 100 \quad (7)$$

Where, ΔL is the difference in the measured length of the specimen (mm), L_0 is the reference rod gauge length (mm)

2.6.2 Water Absorption and Porosity

The second parameter under durability studies adopted is water absorption and porosity to assess the permeability and pore structure of the concrete. The water absorption test was conducted

following the guidelines provided in IS 2386 Part III: 1963 to evaluate the capacity of the concrete to absorb water under standard conditions [63]. The cubes of 100 mm x 100 mm x 100 mm were oven dried for 24 hours and then immersed in water for the next 24 hours. Dry and wet weights (M_{dry} and M_{sat}) were taken to compute the water absorption after 28 days of curing for each mix using Eq. (8). The porosity on the cubical specimens was measured as per code DIN 1048 so as to comprehend the process of water transport within the pore structure and to estimate the linked pore space after 28 days of curing of all the different specimens using Eq. (9).

$$\text{Water absorption (W)} = \frac{\text{Msat}-\text{Mdry}}{\text{Mdry}} \text{x100} \quad \text{(expressed in \%)} \tag{8}$$

$$\text{Porosity (P)} = \frac{\text{Msat}-\text{Mdry}}{\rho_w \text{ x V}} \text{x100 (expressed in \%)} \tag{9}$$

Where, M_{dry}=Oven dry weight of cubes (g); M_{sat}= after 24 hours wet weight of cubes (g)

2.7 Crack Healing Assessment

Concrete fissures play a crucial role in long-term performance in structural integrity and durability. Due to the self-healing mechanisms, there can be a reduction in the crack width; the crack can be sealed without any human intervention through an autonomous mechanism [6, 33, 64, 65]. In this study, crack closure assessment was conducted systematically to quantify the effect of bacterial agents and calcium-based nutrients on crack repair over time.

Fig. 6. Cracks inducing on the specimens using a CTM and b. Microscope used for the crack closure assessment

The crack healing quantification was performed by initially inducing the pre-crack by applying gradual loading (~100 kN) using CTM until the crack appeared on the surface of the concrete specimen after 28 days of water curing to ensure proper hydration [66, 67]. Care was taken to avoid overloading the specimens to ensure the cracks were well-defined but did not compromise the structural integrity of the concrete. To replicate real-world conditions, the induced cracks varied in width, ranging from approximately 0.1 mm to 4 mm. The microscope crack width detector with an optical magnification of X40 (manufactured by C&D Microsystem Limited, UK) (Fig. 6) was employed to precisely measure the initial crack widths. The specimens were further immersed in the curing tank for a period of 28 and 91 days. Each crack's width was measured at multiple points along its length to account for variability, and the maximum crack width closure was recorded on the aforementioned days of curing.

2.8 Microstructural Analysis of The Crack-Healed Sample

Microstructural analysis was conducted using SEM, XRD, and FTIR to understand bacterial concrete's microstructural changes and self-healing capabilities thoroughly at the microscale level to quantify the phase composition, crystal morphology, and chemical bond identification during the process of healing [28, 68-71]. SEM coupled with EDS was performed to capture high-resolution micrographs of the concrete's surface and the interfacial transition zones (ITZ). Samples were

fractured in order to expose fresh surfaces and allowed to dry. The SEM model named TESCAN MIRA S6123 comprises secondary electron mode (SE) was operated at an accelerating voltage of 15–20 kV, beam landing energy of 0.2 to 30 KeV and images were taken at magnifications ranging from 1000 to 5000X to provide detailed morphological observations, identifying the phases, and visualization of crack healing calcite precipitation. XRD analysis was conducted to identify the mineralogical phases in the bacterial concrete, specifically the polymorphs of calcium carbonate such as calcite, aragonite, and vaterite. The XRD instrument used was the Bruker D8 Advance Powder X-ray Diffractometer, which operates with Cu Kα radiation at a wavelength of 1.5418 Å. The finely powdered samples (particle size below 45 μm) were scanned over a 2θ range of 10° to 80° to generate diffraction patterns. FTIR was employed to identify and characterize the chemical bonds and functional groups present in the concrete samples, mainly focusing on bio-mineralization products such as calcium carbonate ($CaCO_3$). The analysis was conducted using the Bruker ALPHA-II ATR-FTIR Spectrophotometer. It is equipped with a zinc selenide (ZnSe) beam splitter and a high-resolution deuterated triglycine sulfate (DTGS) detector. The FTIR spectrum was recorded in the wavenumber range of 4000 cm^{-1} to 500 cm^{-1}, with an air-cooled IR source operating at 12V and 20W. Approximately 5 mg of the powdered sample was placed on the ATR crystal to ensure optimal surface contact, eliminating the need for additional sample preparation, such as pellet formation.

2.9 Statistical Analysis

The data were analyzed by analysis of variance (ANOVA) followed by Tukey's honestly significant difference (HSD) test to assess the significance of differences between the variances using Origin Pro 8.5 software. In each graph plotted, the error bars represent the standard deviation, and they remained less than 0.05 %. The data was found to be significantly different at $p<0.05$.

3. Results and Discussion

3.1 Bacterial Preparation and Characterization

The results obtained from the microbiological investigation of *B. subtilis* confirm its suitability for self-healing concrete applications. The bacterium's morphological, enzymatic, and growth characteristics were evaluated comprehensively, and its performance was analyzed in the context of its role in promoting calcium carbonate precipitation.

3.1.1 Morphological Characterization of Bacteria

The Gram staining analysis revealed the rod-shaped morphology of *B. subtilis* with purple staining, confirming its Gram-positive nature (Fig. 7a). The endospore staining revealed the presence of both vegetative cells and endospores in the *B. subtilis* culture. Under microscopic observation, the vegetative cells appeared pink. At the same time, the endospores were distinctly stained green (Fig. 7b), confirming the bacterium's ability to form endospores under the given conditions, demonstrating adaptability to conditions conducive to calcium carbonate precipitation.

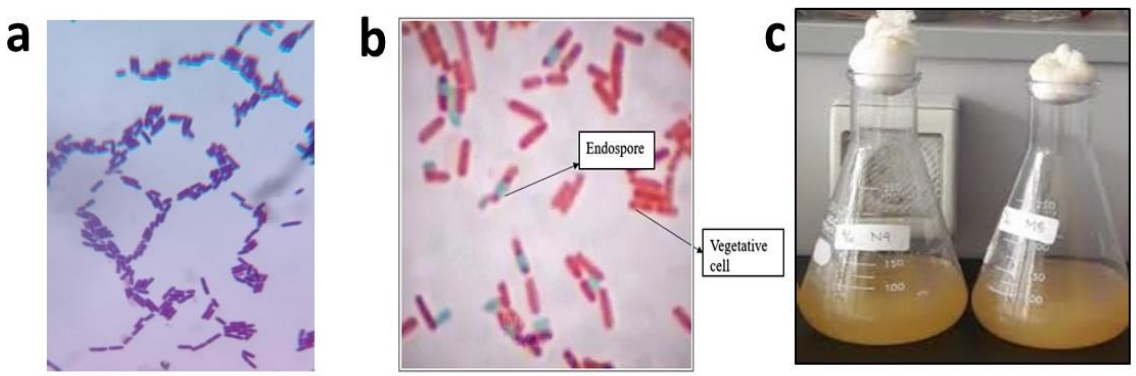

Fig. 7. (a) Microscopic image of *B. subtilis* (b) Endospores staining of *B. subtilis* and (c)Inoculated broth after 24 h incubation

The rod-shaped morphology of the bacterium, and in particular its ability to form endospores, supports its structural durability and survivability against harsh and alkaline environments in the concrete matrix. The bacterial spores thrived at 37 °C and pH 11 on nutritional agar media (Fig. 7c). Its ability to continue growing in these circumstances is essential to its self-healing concrete functioning. Its functionality in self-healing concrete depends on its capacity to sustain growth in these circumstances.

3.1.2 Urease Test

The urease activity test revealed that *B. subtilis* under the tested conditions, exhibited no hydrolysis of urea. This was evidenced by the absence of any color change within 6 hours, and no significant change was observed even after 24 h of incubation (Fig. 8). These results confirm that *B. subtilis* does not exhibit ureolytic activity, distinguishing it from traditional ureolytic bacteria, which rely on urea hydrolysis for calcium carbonate precipitation [68]. The lack of ureolytic activity positions *B. subtilis* as a non-ureolytic bacterium, making it an environmentally friendlier and potentially more sustainable option for self-healing concrete [1, 49, 72].

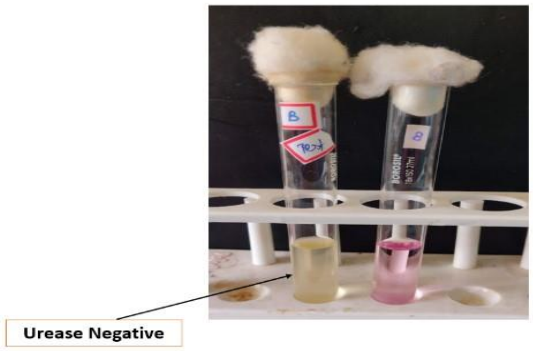

Fig. 8. Urease activity test of *B. subtilis* bacterium

3.1.3 Bacterial Growth Assessment

Robust bacterial growth was promoted by the nutritional broth made with peptone, sodium chloride, HM peptone, and yeast extract. In an orbital shaker incubator set to 30 °C and 148 rpm, the OD measurements, which showed 1.5 after 24 hours of incubation, showed exponential bacterial growth. Calcium formate demonstrated the most effective enhancement of bacterial growth. At 1 % calcium formate, OD peaked at 1.9 after 48 h, maintaining a notable level (1.3) even at 72 h (Fig. 9). This trend remained consistent at higher concentrations: at 2 % calcium formate, OD reached 2.1 (48 h), and at 3 %, it peaked at 2.0 (48 h). These findings demonstrate the metabolic compatibility of calcium formate with *B. subtilis*, which may be because formate is used as an auxiliary carbon source to promote cellular biosynthesis and energy production [73]. Calcium lactate supported a moderate growth at all the concentrations OD values peaked 1.5-1.9. This implies that while lactate might be a source of carbon, *B. subtilis* does not react metabolically to it in the same way that formate does [74, 75].

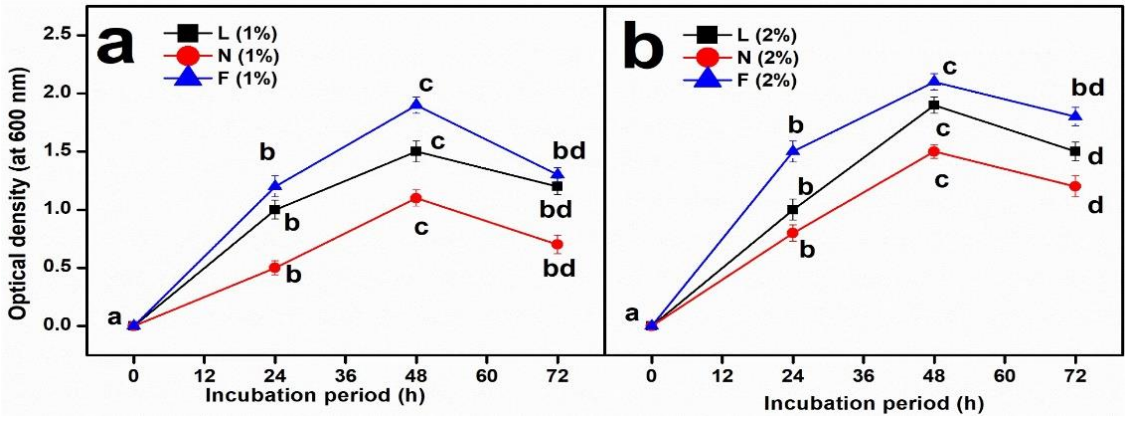

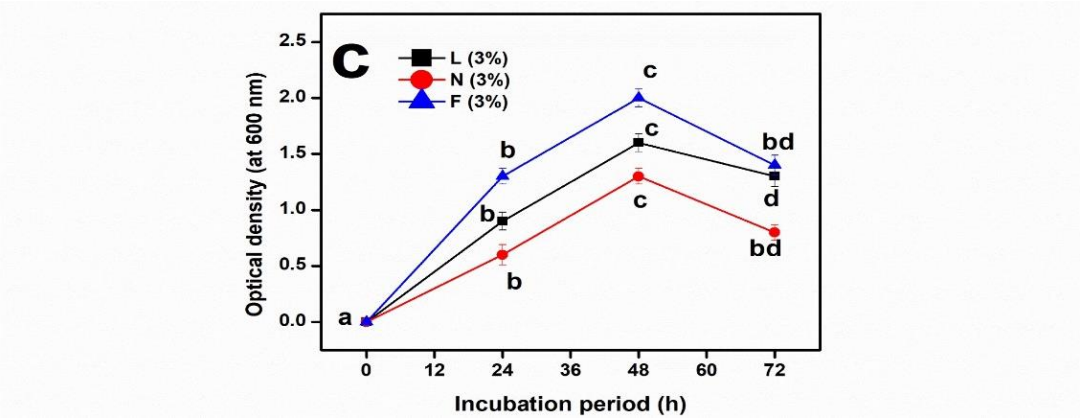

Fig. 9. *B. subtilis* growth with calcium precursors at (a) 1%, (b) 2%, and (c) 3% concentrations. L, lactate; N, nitrate; F, formate. SD < 0.05%; different letters indicate significance at $p < 0.05$ (Tukey's HSD)

In case of calcium nitrate alone, the OD values remained below 1.5 at all concentrations with a peak value of 1.5 at 48 hours at 2% dosage. This finding highlights that *B. subtilis* compatibility with calcium nitrate-based precursors is limited. These findings have been studied from previous studies reported on the implications of bacterial growth in presence of calcium-based precursors [27, 72, 73, 76, 77].

3.1.4 Bacterial Cell Concentration

Hemocytometer-based cell counting determined a spore concentration of 63 cells per 0.1 mm^3 at a dilution factor 10^{-1}. This corresponds to a viable bacterial cell density suitable for application in concrete. The Hemocytometer-based approach provided reliable quantification of bacterial cells, enabling precise incorporation into concrete mixtures. The concentration of bacterial cells in the suspension was determined to be 1.26×10^{-6} cells/mL, experimentally estimated based on OD600 measurements, and a standard calibration curve for *B. subtilis*. This measurement confirms the sufficient cell density for its intended use in MICP processes. The required bacterial medium concentration of 1 x 10^5 cells/mL was maintained in the samples.

3.2 Mechanical Strength: Long-Term Performance Analysis

3.2.1 Compressive Strength Test

As expected, the CC sample exhibited the lowest compressive strength among all mixes due to the absence of supplementary materials or chemical enhancements. At 3 days, the compressive strength was recorded as 14.97 MPa, steadily increasing to 18.27 MPa at 7 days, reaching 33.83 MPa at 28 days, and finally plateauing at 44.52 MPa at 91 days. The calcium lactate series demonstrated significantly enhanced compressive strength values compared to the CC mix. For instance, (1BC-L) mix achieved a strength of 33.27 MPa at 3 days, nearly doubling the value of CC mix (Fig. 10a). The increased strength is attributed to the presence of precursors that accelerate the hydration process and improve particle packing [78, 79]. A strength of 53.5 MPa was obtained by the (1BC-L) mix after 91 days, demonstrating sustained pozzolanic action. 2BC-L and 3BC-L also showed similar patterns, but with 3BC-L mix, somewhat lower values were depicted as the materials embedded in the cement matrix don't undergo proper hydration [21, 79-81]. The calcium nitrate series demonstrated superior performance, particularly at later curing ages. 2BC-N represented the highest strength amongst three dosages, achieving to 57.15 MPa at 91 days (Fig. 10b). The improvement is attributed to the crystalline admixture's ability to refine the pore structure, The microstructural densification from the crystalline material's self-healing capabilities contributed significantly to the improved mechanical properties [30, 82-84]. The development of compressive strength was found to be greatly impacted by the calcium formate series. The most pronounced enhancement became apparent at 3% dosage of calcium formate, achieving 37 MPa and a noteworthy of 62 MPa at 91 days (Fig. 10c). This improvement is attributed to the calcium formate ability to undergo crack control mechanism and compounded stress distribution evenly

within the matrix. These findings are in line with the studies that exhibited the efficiency of calcium formate in increasing the strength and effectiveness in crack mitigation [32, 85, 86].

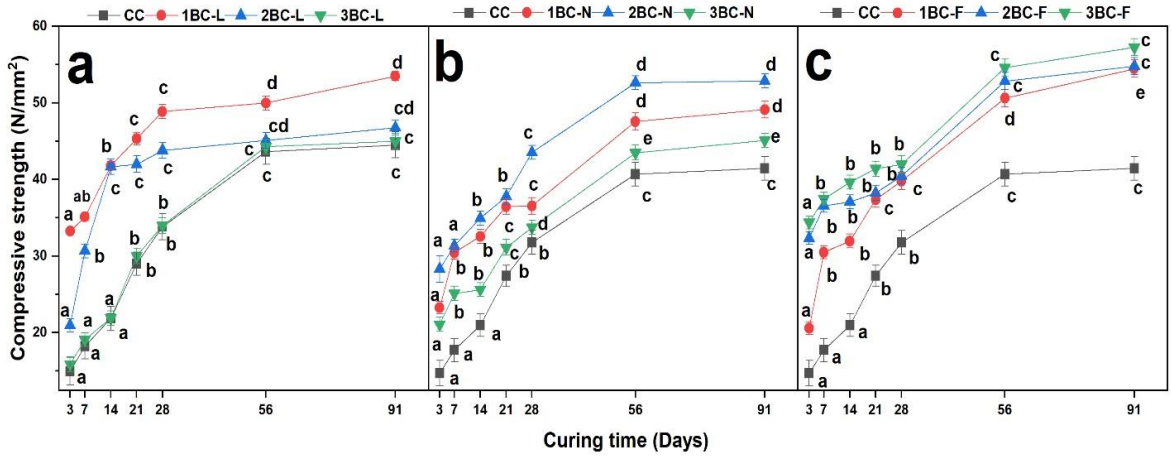

Fig. 10. Compressive strength of bacterial concrete with (a) calcium lactate, (b) calcium nitrate, and (c) calcium formate at 1%, 2%, and 3% dosages. CC: control; BC-L/N/F: bacterial concrete with respective precursors. SD < 0.05%; different letters indicate significance at $p < 0.05$ (Tukey's HSD)

3.2.2 Flexural Strength Test

A systematic evaluation of the impact of all three calcium sources on concrete's flexural strength was conducted. (1BC-L) mix, amongst the other two, exhibited the best performance across all curing ages. It achieved a flexural strength of 5.58 MPa at 91 days, significantly higher than that of the conventional concrete mix (CC, 4.5 MPa) (Fig. 11a). Additionally, it is attributed to the optimal performance as there is a balanced release of calcium ions, without causing excessive calcite formation or porosity. Similar findings were established from the earlier studies conducted [79, 87-91]. Calcium nitrate at 2% dosage (2BC-N) mix outperformed the other mixes for calcium nitrate-based systems, achieving a strength of 5.5 MPa at 91 days (Fig. 11b). This consistent improvement in flexural strength highlights the role of calcium nitrate as a hydration accelerator.

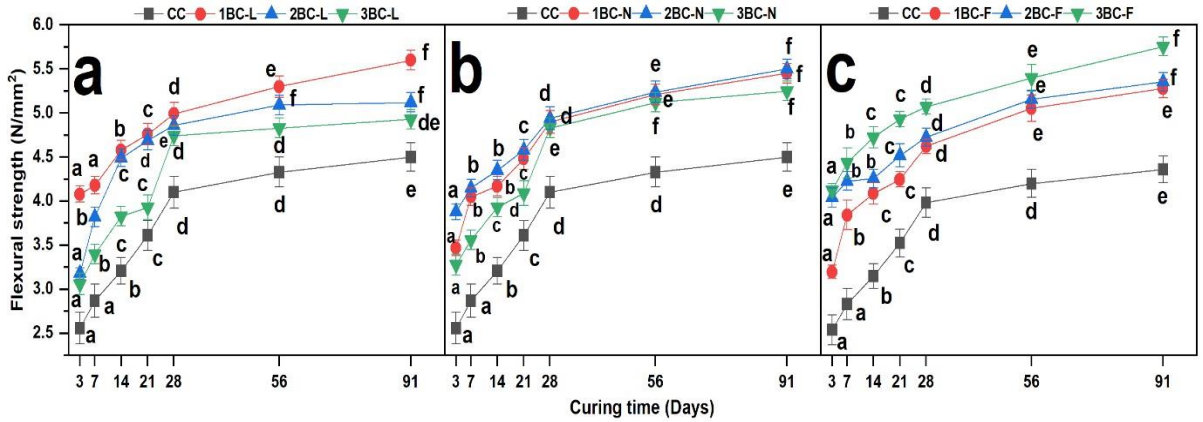

Fig. 11. Flexural strength of bacterial concrete with (a) calcium lactate, (b) calcium nitrate, and (c) calcium formate at 1%, 2%, and 3% dosages. CC: control; BC-L/N/F: bacterial concrete with respective precursors. SD < 0.05%; different letters indicate significance at $p < 0.05$ (Tukey's HSD)

However, both lower (1BC-N) mix and higher (3BC-N) mix concentrations showed relatively inferior results, with the (3BC-N) mix demonstrating a slight decline in long-term strength, potentially due to localized hydration reactions leading to uneven microstructural distribution [29, 92-94]. Mixes embedded with calcium formate displayed the most significant early-age strength gains. (3BC-F) mix achieved 4.25 MPa at 3 days and reached 5.99 MPa at 91 days (Fig. 11c), making

it the best-performing individual precursor across all curing ages. The high efficiency of the (3BC-F) mix is attributed to its dual role as a hydration accelerator and ITZ (interfacial transition zone) densifier. The presence of formate ions facilitated rapid calcium silicate hydrate (C-S-H) gel formation, which improved both early and long-term strength [32, 86, 95].

3.2.3 Split Tensile Strength

The effects of the three calcium sources on the split tensile strength of concrete were systematically assessed. Compared to all the mixes inclusive of calcium lactate, mix with 1% dosage of calcium lactate established an improvement at all curing periods (Fig.12a). At 91 days, (1BC-L) mix achieved a split tensile strength of 4 MPa, substantially higher than the control mix (CC), which registered 3 MPa. The balanced ionic release of calcium lactate in (1BC-L) mix likely contributed to uniform hydration and strength improvement. Higher concentrations, such as (3BC-L) mix, showed moderate increases in tensile strength (3.35 MPa at 91 days), potentially limited by residue build up and increased porosity caused by surplus ions. Several studies demonstrate similar findings to those shown in the current study [75, 79, 87, 88, 96]. Amongst the calcium nitrate-based mixes, (2BC-N) mix performance imputed acceleration properties of calcium nitrate, which facilitated matrix densification and enhanced bonding between aggregates and cement paste (Fig.12b). Conversely, (3BC-N) mix exhibited a slightly lower tensile strength of 3.75 MPa at 91 days due to over-acceleration of hydration. These findings were in line with the previous studies reported by the incorporation of calcium nitrate [92, 93, 97]. Bacterial concrete mix embedded with calcium formate substantial early-age strength enhancements, with (3BC-F) mix standing out as the best-performing individual precursor. At 91 days, (3BC-F) mix achieved a tensile strength of 4.11 MPa (Fig.12c), demonstrating its efficiency as a hydration accelerator and microstructure densifier [82, 85].

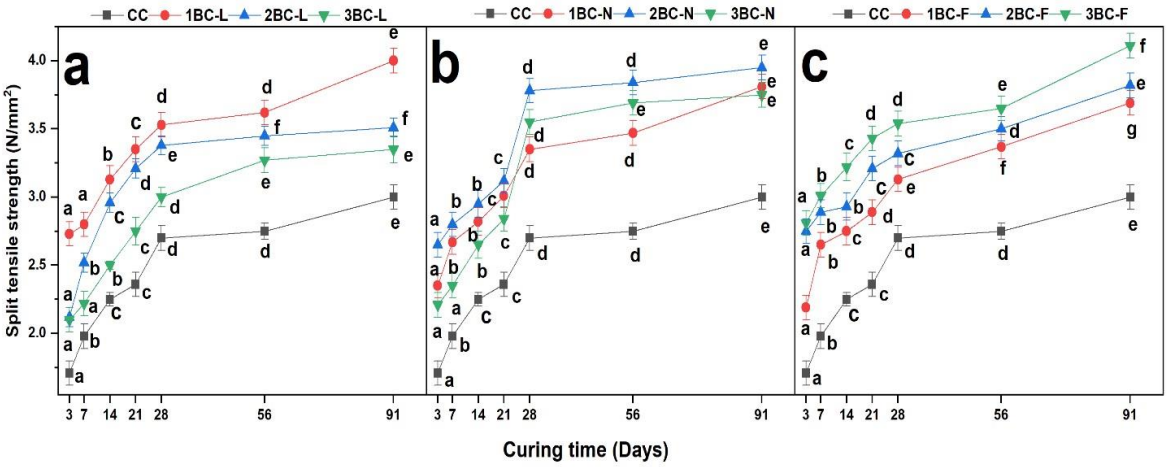

Fig. 12. Split tensile strength of bacterial concrete with (a) calcium lactate, (b) calcium nitrate, and (c) calcium formate at 1%, 2%, and 3% dosages. CC: control; BC-L/N/F: bacterial concrete with respective precursors. SD < 0.05%; different letters indicate significance at $p < 0.05$ (Tukey's HSD)

3.3 Durability Parameters

3.3.1 Drying Shrinkage

The drying shrinkage values for different concrete mixtures over 7, 35, and 91 days under sun-drying and moist-drying conditions give insight into how calcium-based precursors affect shrinkage performance, as shown in Table 3**.** Cement mortar mix showed relatively low drying shrinkage under both sun-drying (0.815 %) and moist-drying conditions (0.532 %). In the presence of mortar samples embedded with bacterium medium and calcium precursors exhibited an increase in shrinkage was observed at 7 days [55]. Bacterial mortar mixes such as (1BC-L) mix and (1BC-N) mix exhibited the highest shrinkage under sun-drying conditions at 1.363 % and 2.297 %, respectively. Under moist-drying conditions, the (1BC-N) mix displayed the highest shrinkage at

3.607 %. By 35 days, the trend showed significant shrinkage reductions across all mixes compared to the 7-day results. Mortar mix exhibited a shrinkage of 0.402 % (sun-dry) and 0.319 % (moist-dry). Bacterial mortar mix such as (3BC-L) and (2BC-N) achieved moderately lower shrinkage values under sun-drying (0.146 % and 0.471 %, respectively) compared to the earlier stages, indicating the mitigation of shrinkage effects with time, and these are aligning with the findings of [11, 98, 99]. At 91 days, drying shrinkage established stabilized values, casting minimal difference values under both drying conditions. Mortar mixes depicted values of 0.335 % (sun-dry) and 0.450 % (moist-dry), suggesting consistent behavior over time. Interestingly, bacterial mortar mixtures with higher calcium source dosages, such as (3BC-L), and (3BC-F) demonstrated minimal shrinkage values of about 0.079 % and 0.026 % and 0.103 % and 0.335 % under sun-dry and moist-dry conditions, respectively [32]. The results indicate that calcium-based nutrients significantly affect the drying shrinkage of concrete. The increase in 7-day observation is attributed to the high reactivity of the calcium precursors that accelerated more loss in moisture content due to enhanced hydration process, as supported by several research studies [32, 85, 89, 100]. The current study confirms that at an early age, shrinkage amplification necessitates careful consideration of dosage and curing conditions to balance performance outcomes. However, at higher concentrations, they mitigate the long-term shrinkage effect [101]. The standard deviation was less than 0.05 %. Means followed by letters are significantly different at $p < 0.05$ according to Tukey's HSD test.

Table 3. Drying shrinkage of conventional concrete and bacterial concrete using calcium precursors.

Mortar Mix Type	7th Day		35th Day		91st Day	
	Sun Dry	Moist Dry	Sun Dry	Moist Dry	Sun Dry	Moist Dry
Cement mortar	0.815^{a}	0.532^{a}	0.402^{a}	0.319^{a}	0.335^{a}	0.450^{a}
1BC-L	1.363^{b}	1.483^{b}	0.430^{a}	0.445^{b}	0.263^{a}	0.332^{a}
2BC-L	1.048^{c}	1.800^{c}	0.750^{b}	0.753^{c}	0.249^{a}	0.107^{b}
3BC-L	0.896^{a}	1.830^{c}	0.146^{c}	0.549^{b}	0.079^{b}	0.103^{b}
1BC-N	2.297^{d}	3.607^{d}	0.465^{a}	0.487^{b}	0.223^{a}	0.216^{c}
2BC-N	1.530^{e}	1.732^{c}	0.471^{a}	0.191^{d}	0.070^{b}	0.119^{b}
3BC-N	0.863^{a}	1.900^{c}	0.492^{a}	0.605^{e}	0.397^{a}	0.403^{a}
1BC-F	2.005^{f}	1.441^{b}	0.297^{d}	0.617^{e}	0.094^{b}	0.314^{a}
2BC-F	2.098^{f}	1.500^{b}	0.558^{a}	0.422^{b}	0.346^{a}	0.001^{b}
3BC-F	3.103^{g}	1.400^{b}	0.267^{d}	0.500^{b}	0.026^{b}	0.335^{a}

3.3.2 Water Absorption and Porosity

Two essential metrics for evaluating the durability and permeability qualities of concrete are water absorption and porosity. These properties directly affect the long-term structural performance and service life of concrete and control its vulnerability to environmental degradation [79, 102]. The conventional concrete mix (CC) exhibited a water absorption of 2.7 % and porosity of 7 %. These values represent the baseline for comparison with bacterial-based concrete mixes. (1BC-L) mix showed reduced water absorption (2.36 %) and porosity (6.3 %) compared to CC, indicating enhanced durability due to the densification of the microstructure [36]. (2BC-L) mix and (3BC-L) mix exhibited higher values of water absorption (3.34 % and 3.6 %, respectively) and porosity (8.52 % and 9.59 %), which may be attributed to the dosage of calcium lactate influencing hydration and void formation [103].

The results demonstrate that a controlled dosage of calcium lactate can reduce porosity and improve the water-tightness of concrete. (1BC-N) mix and (2BC-N) mix had moderate water absorption values (3.2 % and 2.96 %) and porosity (8.5 % and 7.4 %), suggesting slight improvements in durability compared to CC. (3BC-N) mix exhibited the highest water absorption (3.8 %) and porosity (10 %), likely due to increased voids or inconsistent hydration effects at higher calcium nitrate dosages. These results emphasize the need for optimization of calcium nitrate dosage to achieve a balanced microstructure with reduced porosity.

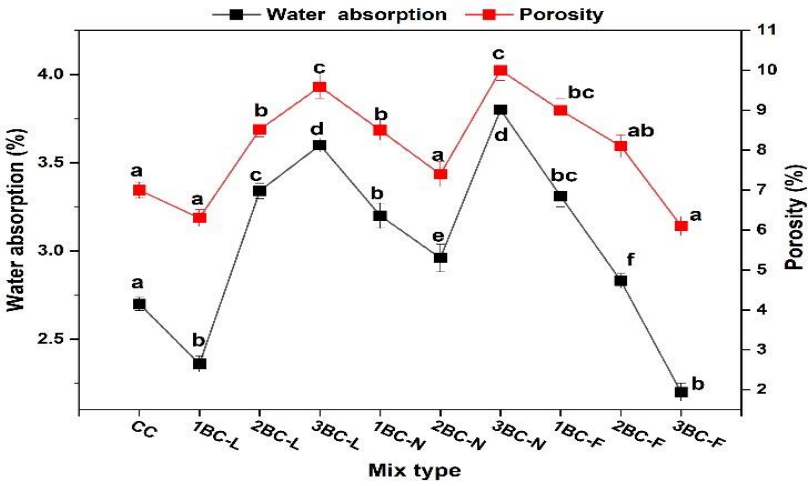

Fig. 13. Water absorption and porosity of conventional and bacterial concrete. SD < 0.05%; different letters indicate significance at p < 0.05 (Tukey's HSD).

The calcium formate mixes demonstrated good performance in terms of water absorption and porosity. (1BC-F) mix and (2BC-F) mix had slightly elevated water absorption values (3.31 % and 2.83 %, respectively) with 9 % and 8.1 % corresponding porosities. (3BC-F) mix exhibited the lowest water absorption (2.2 %) and porosity (6.1 %) among all calcium formate mixes (Fig.13) highlighting its potential for enhancing concrete durability. The performance of (3BC-F) mix indicates that calcium formate, when used in optimal amounts, effectively reduces voids and water ingress. Earlier research has demonstrated that calcium-based precursors such as calcium lactate, calcium nitrate and calcium formate significantly impact concrete's water absorption and porosity [32, 52, 94, 101, 104, 105].

3.4 Performance of Cracks' Self-Healing in Concrete

Cubical specimens (100 x 100 mm), one each of all mixes, including conventional concrete, were cast for examining the crack healing performance. (Fig.14) and (Fig.15) depicts the appearance of the induced pre-crack width and healing of the micro-cracks respectively due to the formation of calcite precipitation, which was observed using a Microscope crack width detector with optical magnification of 40X (C & D Microsystem Limited, UK). In a study performed on cement paste prismatic specimens where artificial cracks of about 1 mm were developed, the closure of a 0.8 mm crack width was reached after 20 days of repairing [106]. Calcium lactate at 1% dosage exhibited minimal induced pre-crack width compared to the other two dosages. Induced pre-crack width increased with an increase in dosage of calcium lactate. The complete healing of the induced pre-crack width was observed at 91 days at all dosages of calcium lactate. More amount of increased calcite formation with an increase in dosage was observed in case of calcium lactate as precursor. Although the higher dosages of calcium lactate enhance the calcite precipitation and aid in pore filling and healing of the crack width, excessively higher concentrations lead to a reduction in compressive strength, increasing the porosity of the concrete matrix before crack formation. Low concrete strength, with an increase in porosity, results in a more fragile matrix, which in turn leads to the development of wider induced pre-crack width under the application of gradual loading [81, 107]. Certain findings on crack healing depicted that in presence of calcium lactate 0.46 mm of crack closure using bacterium *B. alkalinitrilicus* [64]; with alkali resistant *B. subtilis* M9, bearing the calcium lactate medium and alcohol fibres 0.3 mm crack was created at bottom of the beam was evaluated with aid of SEM observation [108]. Both the mixes in the presence of spores and cultured form resulted in good healing of cracks in a finding [81, 109]. In a study conducted in the presence of *B. pasteurii* solution of 5 x 10^7 cells/mL and calcium lactate solution, when cured in sea-water, showed the maximum efficiency in healing of the crack [110]. The calcium nitrate at 2% dosage showed minimal induced pre-crack width compared to other two nutrients at the same dosages. The maximum induced pre-crack width was observed at 3% dosage and this is in juncture with the porosity developed at this dosage. In a study reported [67], with aid of Thermogravimetric analysis

the filling of the cracks due to $CaCO_3$ was evident in the specimens cast using ureolytic *B. sphaericus* in presence of calcium acetate, calcium nitrate and silica gel. A plain bacterium, either *B. sphaericus or D. nitroreducens,* with the inclusion of nutrients urea, yeast extract, 13.5g calcium nitrate and 9g calcium acetate added in the cement mortar resulted no major impact on the strength parameter [111]. The calcium formate series demonstrated excellent performance, with all mixes (1BC-F, 2BC-F, and 3BC-F) achieving complete closure by 91-day. Calcium formate has depicted a reduction in the induced pre-crack width (1.4 mm) along with the increase in the percentage dosage. This behaviour is attributed to their ability to provide sustained release of healing compounds, promoting continuous hydration and precipitation of calcium carbonate in cracks.

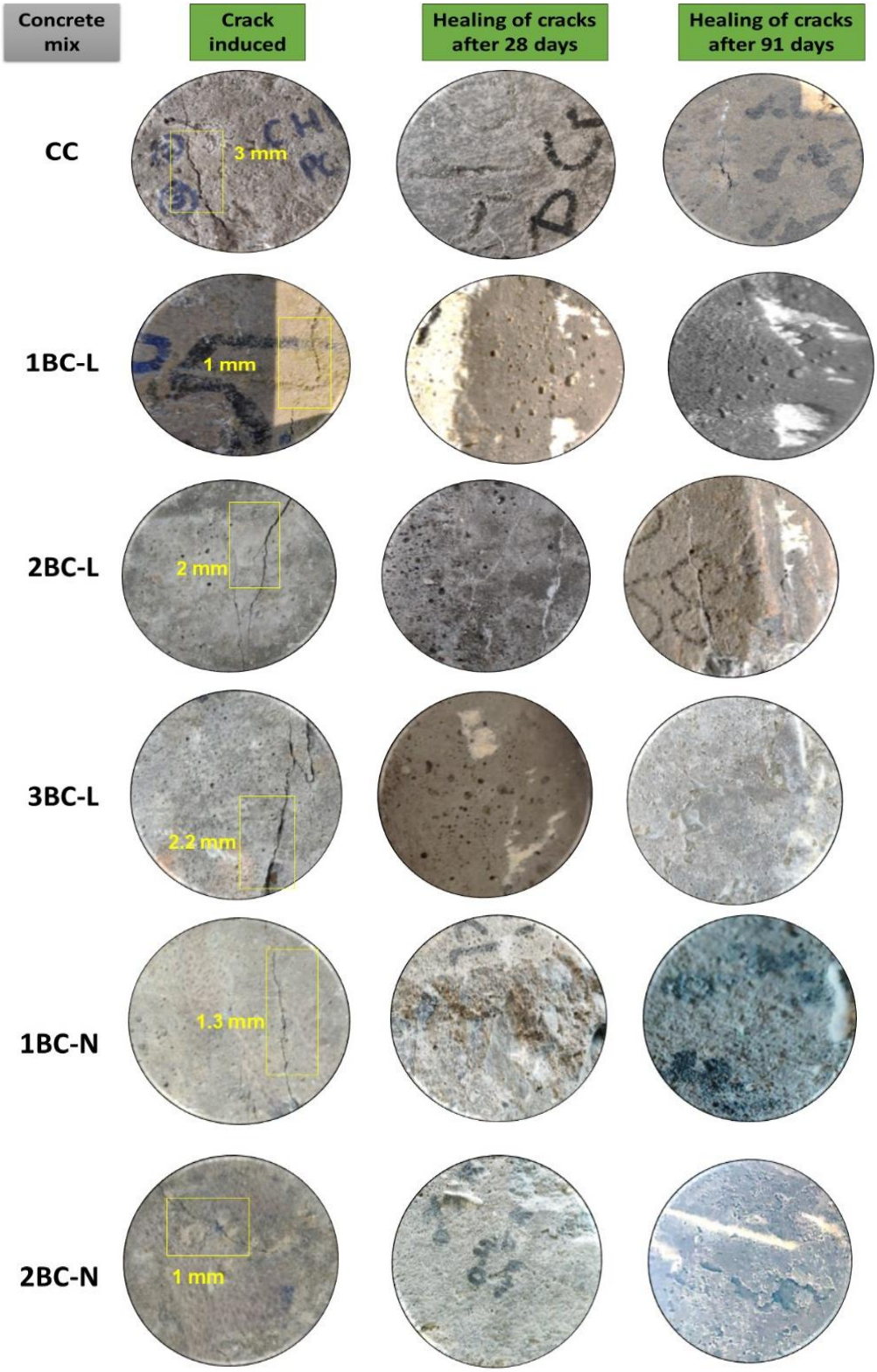

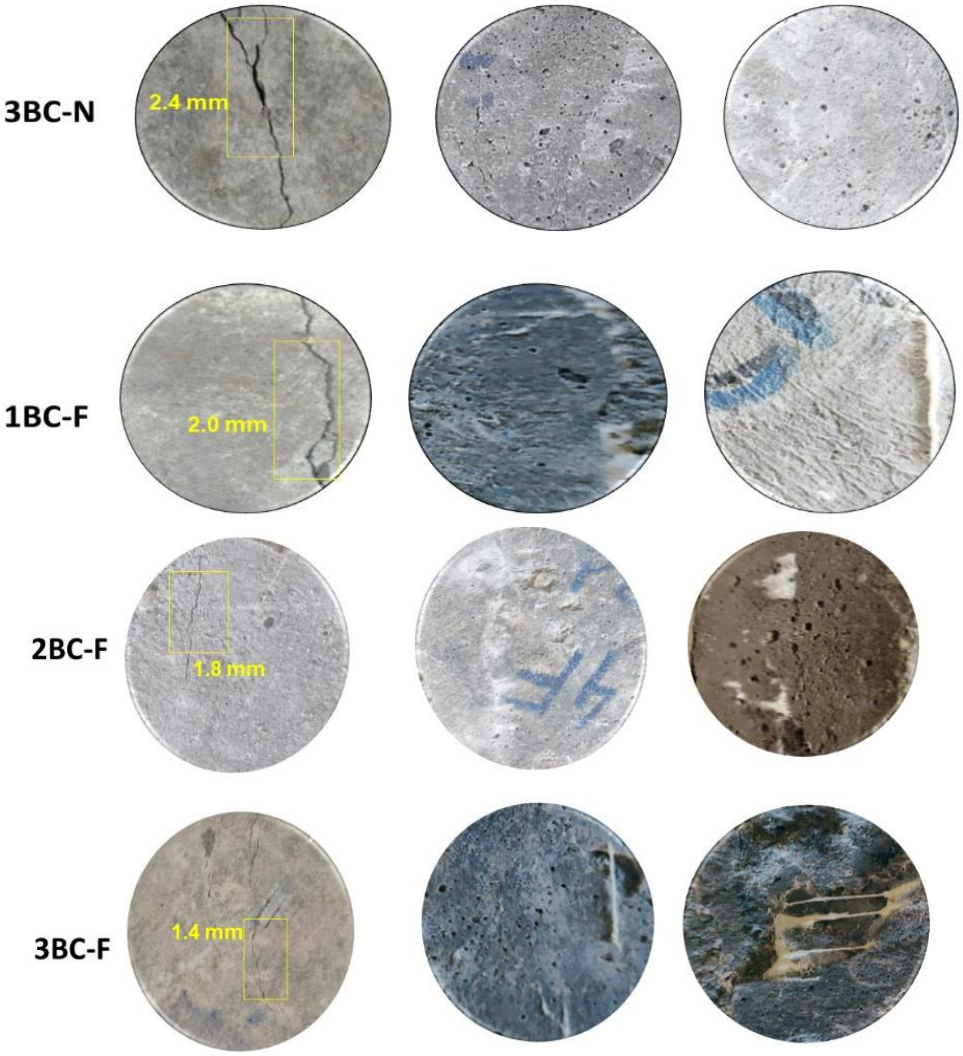

Fig. 14. Crack healing after 28 and 91 days. CC: control; BC-L/N/F: bacterial concrete with calcium lactate, nitrate, or formate at 1%, 2%, and 3% dosages.

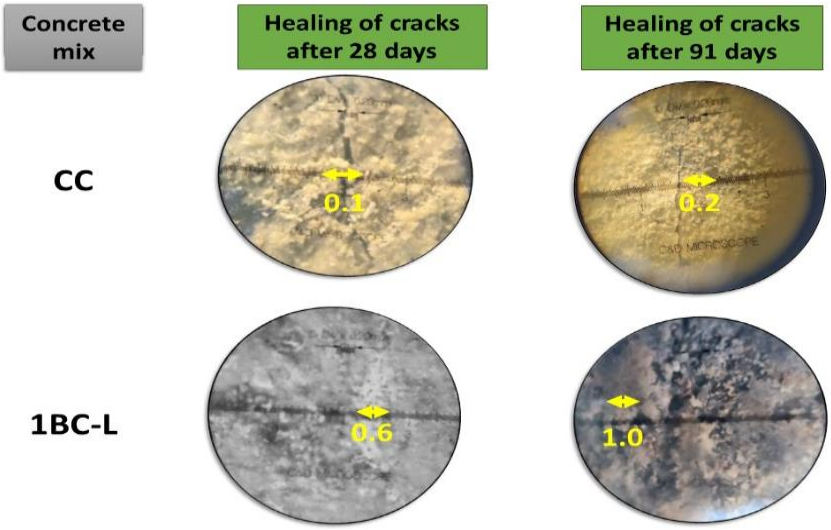

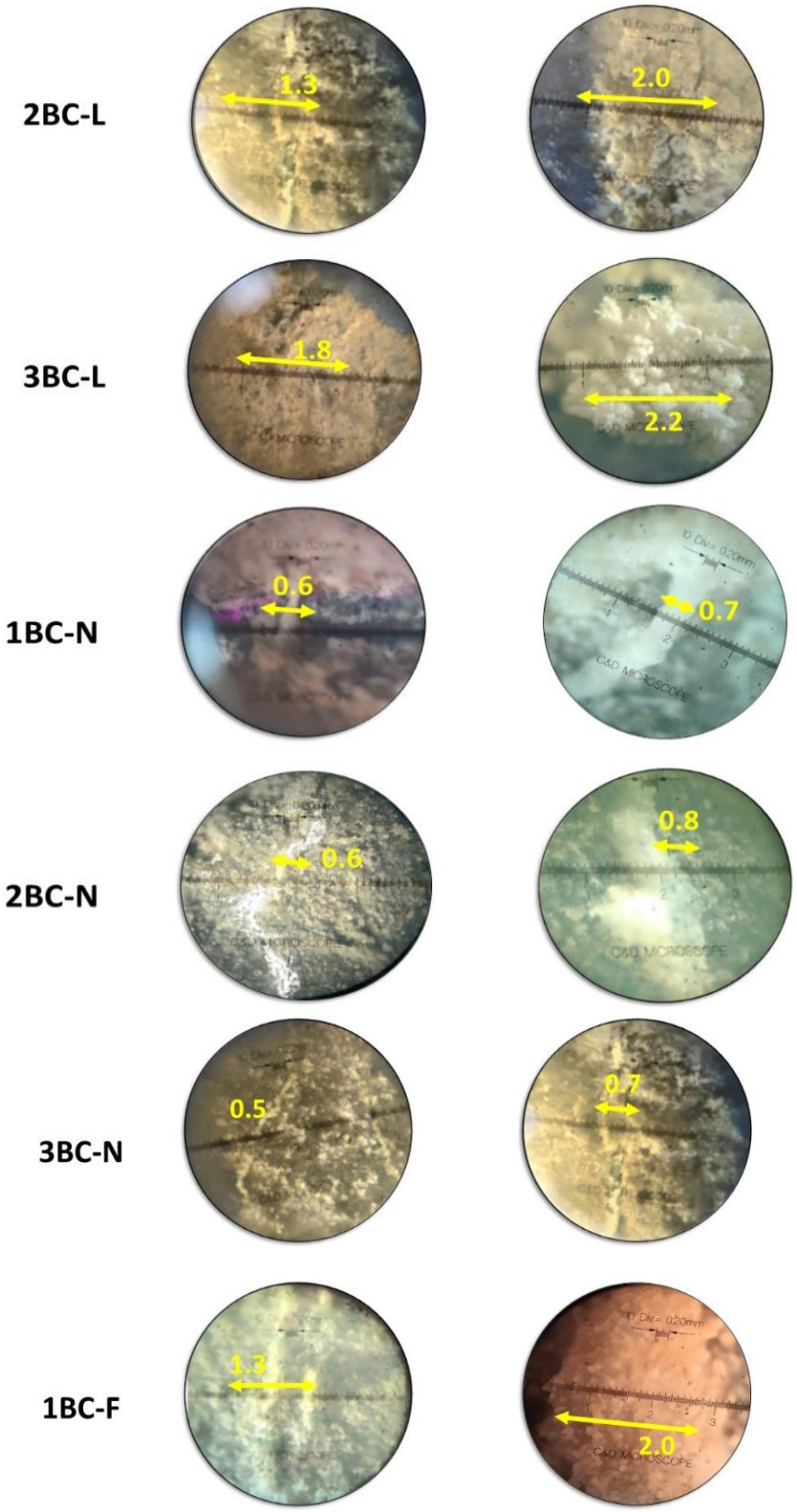
2BC-L
1.3
2.0
3BC-L
1.8
2.2
1BC-N
0.6
0.7
2BC-N
0.6
0.8
3BC-N
0.5
0.7
1BC-F
1.3
2.0

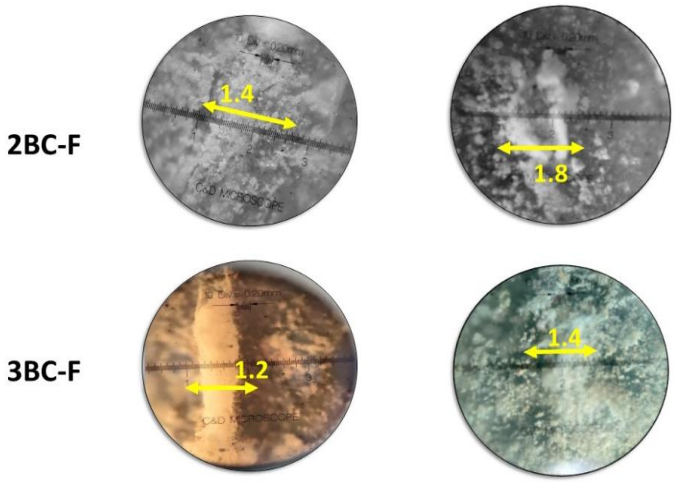

Fig. 15. Microscopic images of crack healing by calcite precipitation after 28 and 91 days. CC: control; BC-L/N/F: bacterial concrete with calcium lactate, nitrate, or formate at 1%, 2%, and 3% dosages.

3.5 Characterization of Materials

3.5.1 Scanning Electron Microscopy (SEM) Equipped with Energy Dispersive X-Ray Spectroscopy (EDS) Analysis

In a way to affirm the formation of MICP in the concrete matrix, SEM analysis was examined on the small size particles and powdered samples of cracked healed specimens after 91 days of healing period. To perform this analysis, conventional concrete (CC) sample specimen and also the bacteria incorporated samples maintaining a required cell concentration of 10^5 cells/mL, with 1% calcium lactate (1BC-L), 2% calcium nitrate (2BC-N), and 3% calcium formate (3BC-F) were preferred as they depicted highest compressive strength. The micrograph from SEM analysis of conventional concrete (CC) specimen revealed a minimal self-healing activity due to presence of limited calcite precipitation along the crack. Formation of the calcite occurred due to the carbonation process and also in presence of certain dispersed hydration products, examined to be small amounts of calcium silicate hydrate (C-S-H) which is the main binding phase appearing as fibrous structure; the by-product cubic C_3A appearing as hexagonal plate-like crystal; and the ettringite compound appearing as needle-like crystals (Fig. 16a). Although portlandite (CH) is present, the absence of substantial calcite deposition or ettringite suggests that the intrinsic healing potential of the conventional concrete is low. (Fig. 16b) represents an SEM image of the bacterial concrete at the required concentration of 10^5 cells/mL, supplemented with 1% dosage of calcium lactate (bwc) (1BC-L). The SEM image shows the formation of calcite($CaCO_3$) crystals along with rod-shaped structure of the *B. subtilis*, particularly along the crack surfaces, in association with bacteria indicated that the bacteria served as a nucleation site during the bio-mineralization process in the presence of precursors [112]. Increased quantities of C-S-H phases and ettringite are evident, suggesting enhanced hydration. Portlandite (CH) and C_3A crystals further corroborate the improved mineral precipitation and contribute to crack closure. (Fig. 16c) represents an SEM image of the bacterial concrete at the required concentration of 10^5 cells/mL, supplemented with 2% dosage of calcium nitrate (bwc) (2BC-N). A substantial growth in ($CaCO_3$) crystal growth and crack closure were apparent in the SEM images. Needle-like ettringite structures were prominently visible, playing a crucial role in sealing cracks and enhancing structural integrity [92]. (Fig. 16d) represents an SEM image of the bacterial concrete at the required concentration of 10^5 cells/mL, supplemented with 3% dosage of calcium formate (bwc) (3BC-F). The SEM analysis of 3BC-F highlights dense calcite formation and abundant C-S-H phases, which effectively fill and seal cracks. The presence of needle-like ettringite and microorganisms embedded within the concrete matrix indicated an active role of microbial activity in biochemical calcite precipitation. The overall microstructure appeared significantly denser compared to that of a conventional concrete specimen. These observations align with previous studies reporting that calcium precursors

improve mineral precipitation and hydration, thereby boosting the self-healing capability of concrete [8, 14, 64, 85, 96, 113-116].

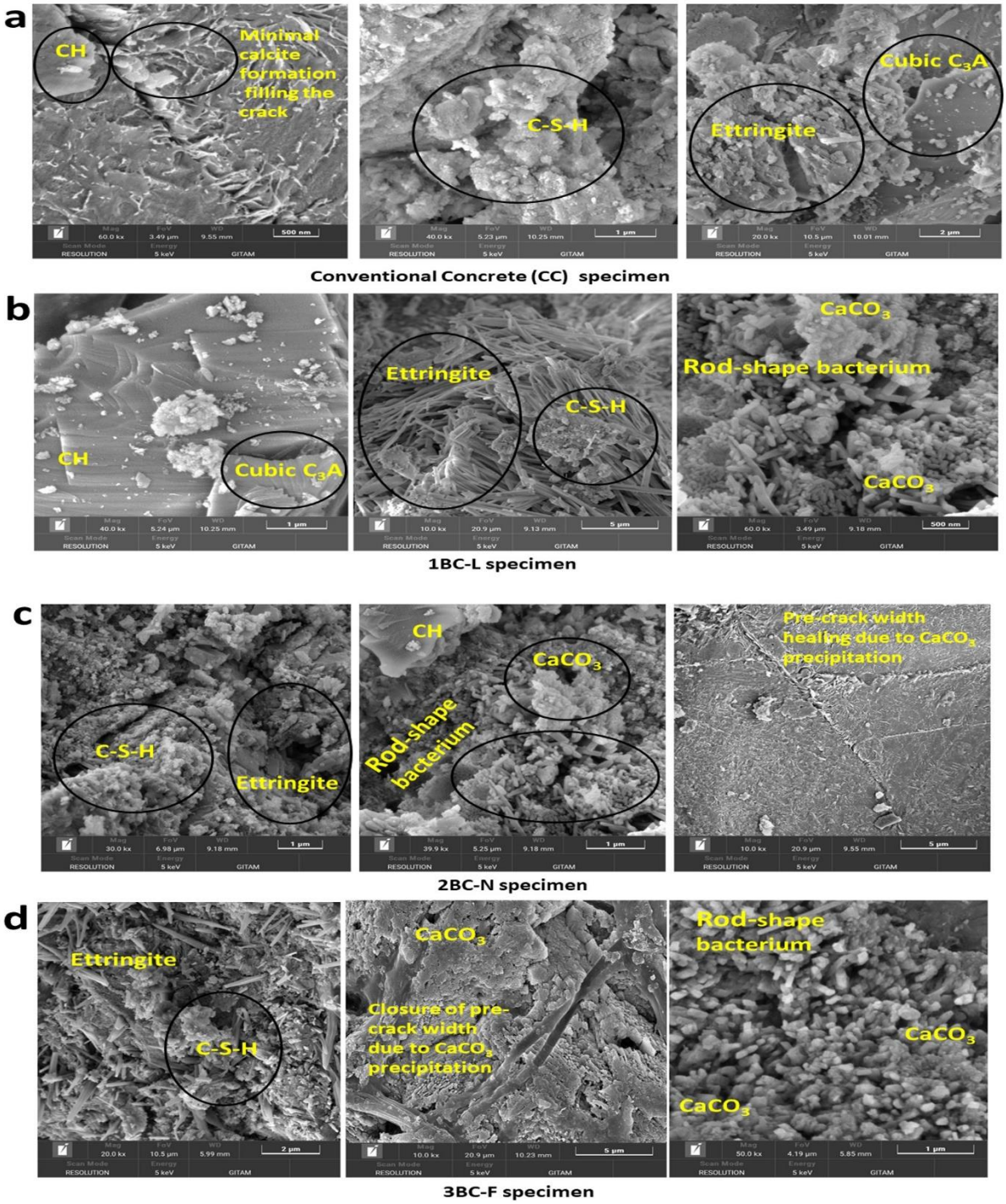

Fig. 16. SEM images of crack-healed concrete after 91 days: (a) CC: control, (b) 1BC-L: 1% calcium lactate, (c) 2BC-N: 2% calcium nitrate, (d) 3BC-F: 3% calcium formate.

Further, EDS provided detailed insights into the chemical constituents responsible for hydration, mineral precipitation, and crack healing. The results complement the microstructural observations from SEM analysis and offer a deeper understanding of the role of calcium-based additives. The EDS spectrum of CC (Fig. 17a) revealed considerable concentrations of oxygen (O, 40.77 wt%) and carbon (C, 25.22 wt%), with moderate levels of calcium (Ca, 18.02 wt%) and nitrogen (N, 4.80 wt%). The high carbon content indicated the limitation in ($CaCO_3$) precipitation, which explains the reduced self-healing potential observed in conventional concrete. (1BC-L) supplemented sample has shown a notable increase in oxygen (O, 44.18 wt %), calcium content (Ca, 30.72 wt %)

with a reduced carbon (C, 19.58 wt %) than CC sample, indicating a notable enhancement in mineral precipitation as shown in (Fig. 17b). The EDS spectrum of 2BC-N supplemented sample (Fig. 17c) has depicted a balanced levels of calcium (Ca, 21.72 wt %), carbon (C, 21.08 wt %), oxygen (O, 43.34 wt %), and nitrogen (N, 4.85 wt %). The increased nitrogen and oxygen levels reflect the beneficial effects of calcium nitrate on hydration and self-healing efficiency. The EDS spectrum of 3BC-F supplemented sample (Fig. 17d) revealed a substantial increase in calcium levels (Ca, 35.89 wt %), oxygen (O, 41.16 wt %), and carbon content (C, 14.96 wt %) is moderately lower than in the other samples, suggesting efficient carbon utilization and indicating robust calcite formation. *B. subtilis* is well-known for its role in calcite formation compared to plain concrete samples, which is similitude in the findings of research studies [5, 21, 24, 117]. These results indicate that calcium formate markedly strengthens the concrete matrix by promoting hydration and mineralization.

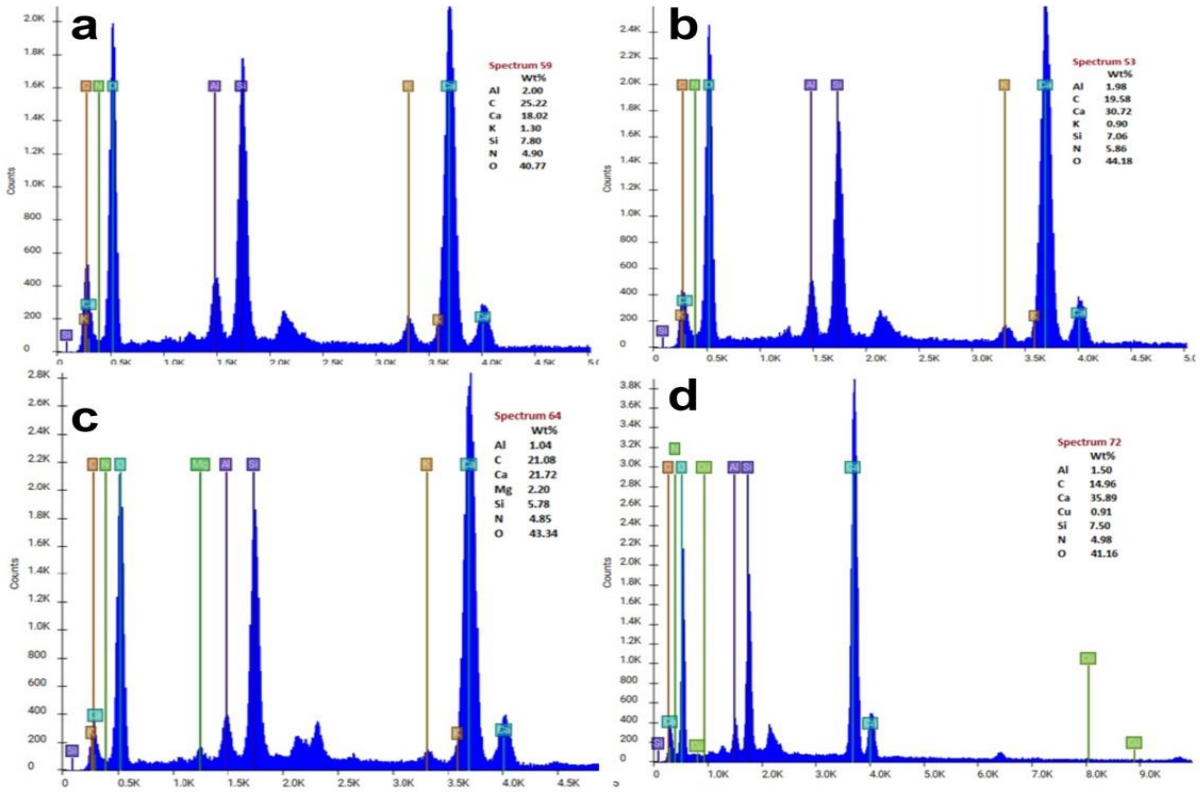

Fig. 17. EDS analysis of crack-healed concrete after 91 days: (a) CC: control, (b) 1BC-L: 1% calcium lactate, (c) 2BC-N: 2% calcium nitrate, (d) 3BC-F: 3% calcium formate.

3.5.2 Powder XRD Analysis of Concrete Samples

The powder X-ray diffraction analysis was performed on both the control and specific bacterial specimens considered for SEM/EDS to observe the cementitious and healing compounds formed in the crack 91 days after healing. The XRD pattern of the CC sample displayed (Fig. 18a) prominent peaks corresponding to calcium silicate hydrate (C-S-H), calcite (C), portlandite (P), and minor peaks of Alite (A) and Belite (B). The dominant peak position of 2Θ for (C) was obtained at 21.5°, indicating its primary role in providing strength to the matrix. Approximately, about (7-10%) the calcium carbonate polymorphs detected in the CC sample were in the form of calcite (C). In case of bacterial concrete samples, amongst the main mineral phases detected by XRD, calcite (C) was predominantly (up to 90%) observed in bacterial samples [118]. The incorporation of (1BC-L) supplemented sample has modified the crystalline profile of the material (Fig. 18b). The XRD pattern revealed an enhancement in calcite (C) formation, as evidenced by the increased intensity of the peak position 2θ at 28.6892°, which confirms its role in filling the pores. The XRD pattern of the sample supplemented with 2BC-N (Fig. 18c) demonstrates a moderate increase in the intensity of C-S-H and calcite (C) peaks. Peaks corresponding to Alite (A), Belite (B), and Portlandite (P) are also observed, but with reduced intensity, possibly due to the conversion of these phases into

secondary hydration products. Concerning the study for pure calcite [119], the highest peak position of 2Θ for calcite (C) was obtained at 26.02435°. The XRD analysis of the sample supplemented with 3BC-F (Fig. 18d) highlights the pronounced formation of calcite (C) and C-S-H. The peaks for secondary phases like Ferrite (F) and Ettringite (E) are more noticeable, suggesting a possible modification in the microstructure due to the formate addition [11]. The broader peaks of C-S-H indicate a possible amorphous nature, contributing to the improved flexibility and self-healing capacity of the matrix. However, the 3BC-F mix has identified the highest peak position of 2Θ for calcite (C) at 29.5°, indicating a pronounced crystallinity in its phase composition and thereby improving the self-healing properties of concrete. These observations align with previous studies indicating that calcium sources enhance mineral precipitation and hydration, thereby improving the self-healing properties of concrete [14, 116, 120, 121].

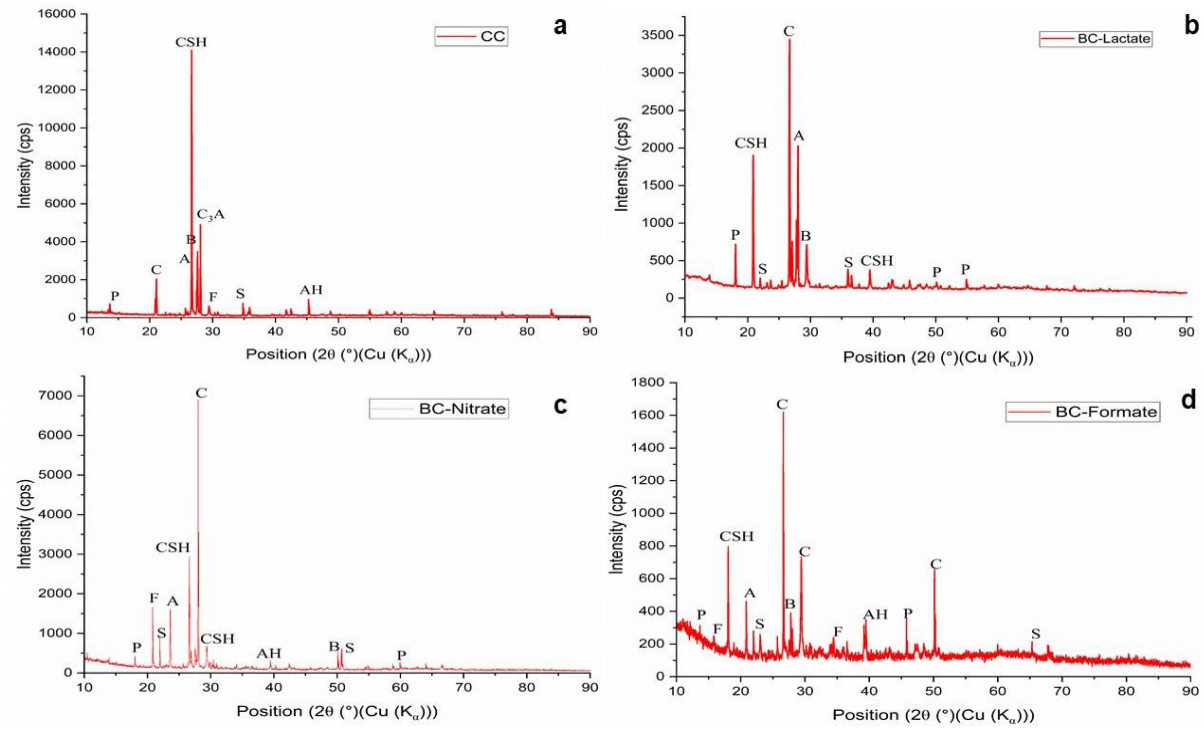

Fig. 18. XRD analysis of crack-healed concrete after 91 days: (a) CC: control, (b) 1BC-L: 1% calcium lactate, (c) 2BC-N: 2% calcium nitrate, (d) 3BC-F: 3% calcium formate.

3.5.3 Fourier Transform Infrared Spectroscopy (FTIR)

FTIR spectroscopy provides critical insights into the chemical interactions and hydration mechanisms in normal and self-healing concrete samples. The FTIR spectrum of conventional concrete (CC) exhibited peaks characteristic of hydration products (Fig.19a). A broad band around 3284 cm^{-1} corresponds to O-H stretching vibrations, signifying bound water in hydrated cement phases such as calcium silicate hydrate (C-S-H) and portlandite ($Ca(OH)_2$) [107, 122-124]. The peak at 1624 cm^{-1}, associated with H-O-H bending vibrations, confirms the presence of adsorbed water. Additionally, the sharp peak near 506–742 cm^{-1} is attributed to Si-O stretching vibrations, which indicate the formation of the primary strength-contributing C-S-H gel. Incorporating calcium lactate into concrete (1BC-L) moderately altered the FTIR spectrum. The O-H stretching band (3350 and 3777 cm^{-1}) intensified, indicating enhanced water retention, while a prominent peak near 1410 cm^{-1} confirmed the presence of carboxylate (COO^-) [123] groups from lactate ions (Fig.19b). The FTIR spectrum of concrete with 2BC-N revealed unique nitrate-associated peaks near 1409 cm^{-1}, indicative of NO_3^- group vibrations. The Si-O stretching band (505-1007 cm^{-1}) showed increased intensity compared to CC, suggesting that calcium nitrate effectively promotes the formation of C-S-H gel [123] (Fig.19c). Self-healing concrete with calcium formate (3BC-F) exhibited a distinct peak at 1408 cm^{-1}, corresponding to the stretching vibrations of formate ions ($HCOO^-$)[11, 123]. The enhancement of Si-O (508-963 cm^{-1}) peaks indicates that calcium formate significantly improves hydration and promotes C-S-H gel formation (Fig.19d).

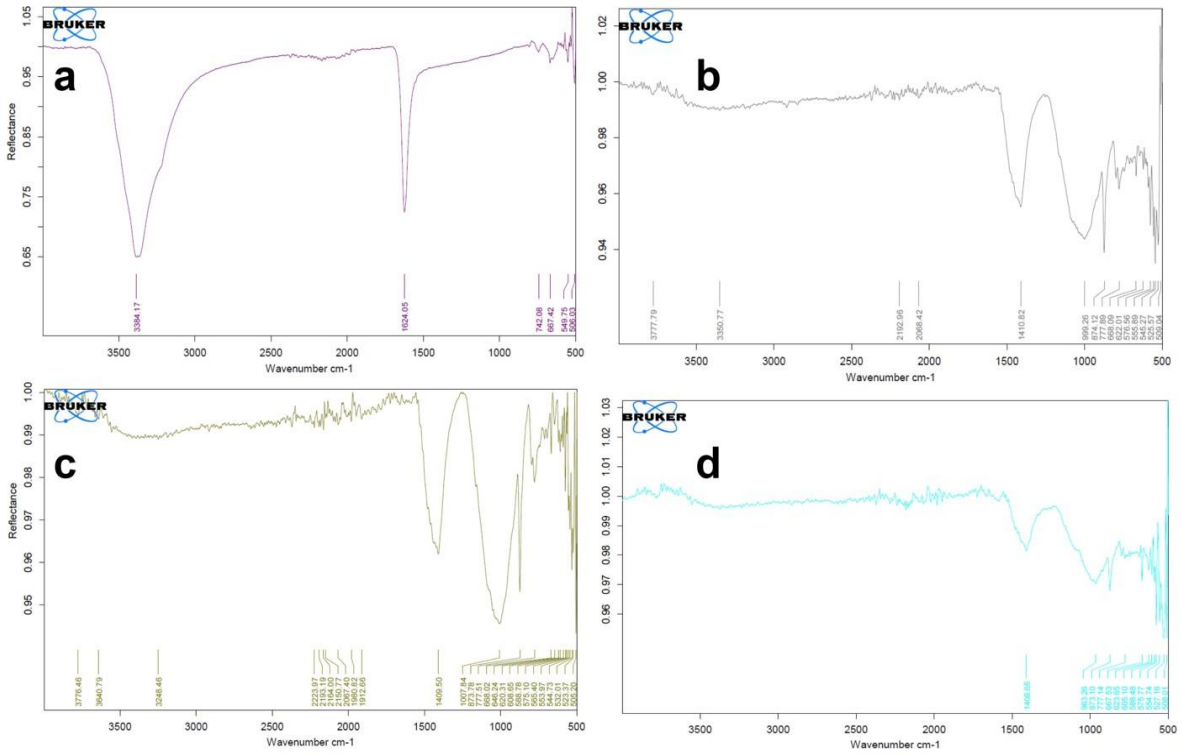

Fig. 19. FTIR analysis of crack-healed concrete after 91 days: (a) CC: control, (b) 1BC-L: 1% calcium lactate, (c) 2BC-N: 2% calcium nitrate, (d) 3BC-F: 3% calcium formate.

4. Conclusions

This current extensive research explains the crucial role of calcium-based precursors in enhancing the mechanical strength properties, durability tests, and autonomous self-healing mechanism of bacterial concrete through the Microbially induced calcium carbonate precipitation (MICP) technique. The experimental setup thoroughly evaluated three different precursors-calcium lactate, calcium nitrate, and calcium formate at varied dosages of (1%, 2%, and 3% by weight of cement) to determine how efficiently they perform in comparison to conventional M20 grade concrete in promoting strength and self-healing properties. The compressive strength evaluation demonstrated that all bacterial concrete formulations successfully retained the target mean strength of M20 grade conventional concrete, with calcium lactate at 1% dosage exhibiting a remarkable increase in strength both at early-age (3-day) and long-term (91-day) hydration periods. Calcium nitrate at 1% and 2% dosages exhibited better resistance characteristics, as it contributes to the densification of the concrete matrix. Conversely, calcium formate at 3% dosage consistently rendered the most substantial mechanical performance improvements, due to its potential in accelerating the C-S-H gel formation and subsequent matrix densification through enhanced bacterial activity. Material characterization techniques, including scanning electron microscopy (SEM) equipped with energy-dispersive X-ray spectroscopy (EDS), powdered X-ray diffraction (XRD), and Fourier-transform infrared spectroscopy (FTIR) rendered detailed insights into the chemical and crystalline phases responsible for self-healing and strength development, such as C-S-H and calcite. The pre-crack width healing evaluation demonstrated that each precursor exhibited distinct capabilities in promoting MICP-mediated healing across varying induced pre-crack widths. Calcium formate at 1% dosage exhibited maximum induced pre-crack width healing performance at both 28 and 91 days of healing period, demonstrating its exceptional capacity to facilitate bacterial proliferation and formation of calcite precipitation within crack interfaces. From the results, it can be concluded that calcium formate is the best nutrient, and it can be applied productively in bacterial concrete to promote and ameliorate the self-healing characteristics. Though in this current study effect of nutrients in the presence of bacteria on concrete parameters has been quantified, certain other factors need to be computed, such as

practical applications of self-healing concrete in real construction works, considering certain environmental conditions such as freeze-thaw cycles, marine exposure, and acidic attack. A detailed optimization study can be conducted for long-term durability effects in the presence of additional additives in order to identify various types of occurrences of cracks. In addition, the cost optimization can also be investigated through a thorough formulation of various calcium sources and their combinations for large-scale applications.

Author Contributions

Material preparation, Casting of Bacterial Concrete, and Testing were performed by [Gouthami Patnaik Palter]. The technical expertise for the manuscript was provided by [Kanaka Durga Sambhana] and [Potharaju Malasani]. The draft of the manuscript was written by [P Gouthami Patnaik]. Microbiological investigations and report were performed by [Venkata Giridhar Poosarla].

References

[1] Tan L, Xu J, Wei Y, Han J, Yao W. Aerobic non-ureolytic bacteria-based self-healing cementitious composites: a novel approach without added calcium precursor. Engineering Research Express. 2023;5(3):035006. https://doi.org/10.1088/2631-8695/ace298

[2] Roig-Flores M, Formagini S, Serna P. Self-healing concrete-what is it good for? Materiales de Construcción. 2021;71(341):e237-e. https://doi.org/10.3989/mc.2021.07320

[3] Seifan M, Samani AK, Berenjian A. Bioconcrete: next generation of self-healing concrete. Applied Microbiology and Biotechnology. 2016;100(6):2591-602. https://doi.org/10.1007/s00253-016-7316-z

[4] De Muynck W, Cox K, Belie ND, Verstraete W. Bacterial carbonate precipitation as an alternative surface treatment for concrete. Construction and Building Materials. 2008;22(5):875-85. https://doi.org/10.1016/j.conbuildmat.2006.12.011

[5] Qian C, Zheng T, Zhang X, Su Y. Application of microbial self-healing concrete: Case study. Construction and Building Materials. 2021;290:123-226. https://doi.org/10.1016/j.conbuildmat.2021.123226

[6] Wang J, Van Tittelboom K, De Belie N, Verstraete W. Use of silica gel or polyurethane immobilized bacteria for self-healing concrete. Construction and Building Materials. 2012;26(1):532-40. https://doi.org/10.1016/j.conbuildmat.2011.06.054

[7] Khoshtinat S. Advancements in Exploiting Sporosarcina pasteurii as Sustainable Construction Material: A Review. Sustainability. 2023;15(18):13869. https://doi.org/10.3390/su151813869

[8] De Muynck W, De Belie N, Verstraete W. Microbial carbonate precipitation in construction materials: a review. Ecological engineering. 2010;36(2):118-36. https://doi.org/10.1016/j.ecoleng.2009.02.006

[9] Worrell E, Price L, Martin N, Hendriks C, Meida LO. Carbon dioxide emissions from the global cement industry. Annual review of energy and the environment. 2001;26(1):303-29. https://doi.org/10.1146/annurev.energy.26.1.303

[10] Palter GP, Syeda M, Sambhana KD, Malasani P, Poosarla VG. A significant review on the performance of microbial concrete in comportment of diverse nutrients. Multidisciplinary Science Journal. 2023;5:2023ss0411. https://doi.org/10.31893/multiscience.2023ss0411

[11] Nodehi M, Ozbakkaloglu T, Gholampour A. A systematic review of bacteria-based self-healing concrete: Biomineralization, mechanical, and durability properties. Journal of Building Engineering. 2022;49:104038. https://doi.org/10.1016/j.jobe.2022.104038

[12] Zhang L, Zheng M, Zhao D, Feng Y. A review of novel self-healing concrete technologies. Journal of Building Engineering. 2024:109331. https://doi.org/10.1016/j.jobe.2024.109331

[13] Li VC, Yang E-H. Self healing materials: an alternative approach to 20 centuries of materials science. S Van Der Zwaag. 2007:161-93.

[14] Althoey F, Zaid O, Arbili MM, Martínez-García R, Alhamami A, Shah HA, et al. Physical, strength, durability and microstructural analysis of self-healing concrete: A systematic review. Case Studies in Construction Materials. 2023;18:e01730. https://doi.org/10.1016/j.cscm.2022.e01730

[15] Abo-El-Enein SA, Ali AH, Talkhan FN, Abdel-Gawwad HA. Application of microbial biocementation to improve the physico-mechanical properties of cement mortar. HBRC Journal. 2013;9(1):36-40. https://doi.org/10.1016/j.hbrcj.2012.10.004

[16] Achal V, Mukerjee A, Sudhakara Reddy M. Biogenic treatment improves the durability and remediates the cracks of concrete structures. Construction and Building Materials. 2013;48:1-5. https://doi.org/10.1016/j.conbuildmat.2013.06.061

[17] Tang Y, Xu J. Application of microbial precipitation in self-healing concrete: A review on the protection strategies for bacteria. Construction and Building Materials. 2021;306:1-11. https://doi.org/10.1016/j.conbuildmat.2021.124950

[18] Xu J, Wang X. Self-healing of concrete cracks by use of bacteria-containing low alkali cementitious material. Construction and Building Materials. 2018;167:1-14. https://doi.org/10.1016/j.conbuildmat.2018.02.020
[19] Xu J, Yao W. Multiscale mechanical quantification of self-healing concrete incorporating non-ureolytic bacteria-based healing agent. Cement and Concrete Research. 2014;64:1-10. https://doi.org/10.1016/j.cemconres.2014.06.003
[20] Wang J, Ersan YC, Boon N, De Belie N. Application of microorganisms in concrete: a promising sustainable strategy to improve concrete durability. Applied Microbiology and Biotechnology. 2016;100(7):2993-3007. https://doi.org/10.1007/s00253-016-7370-6
[21] Vijay K, Murmu M, editors. Experimental study on bacterial concrete using Bacillus subtilis micro-organism. Emerging Trends in Civil Engineering: Select Proceedings of ICETCE 2018; 2020: Springer. https://doi.org/10.1007/978-981-15-1404-3_20
[22] K. Mahmod A, A. Al-Jabbar L, M. Salman M. Bacteria Based Self-Healing Concrete :A Review. Journal of Engineering and Sustainable Development. 2021;25(Special):3-43-3-56. https://doi.org/10.31272/jeasd.conf.2.3.4
[23] Seshagiri R, Reddy VS, Sasikala C. Performance of microbial concrete developed using bacillus subtilis JC3. Journal of The Institution of Engineers (India): Series A. 2017;98(4):501-10. https://doi.org/10.1007/s40030-017-0227-x
[24] Vijay K, Murmu M. Effect of calcium lactate and Bacillus subtilis bacteria on properties of concrete and self-healing of cracks. International Journal of Structural Engineering. 2020;10(3):217-31. https://doi.org/10.1504/IJSTRUCTE.2020.108528
[25] Tobler DJ, Cuthbert MO, Greswell RB, Riley MS, Renshaw JC, Handley-Sidhu S, et al. Comparison of rates of ureolysis between Sporosarcina pasteurii and an indigenous groundwater community under conditions required to precipitate large volumes of calcite. Geochimica et Cosmochimica Acta. 2011;75(11):3290-301. https://doi.org/10.1016/j.gca.2011.03.023
[26] Vaezi M, SAZ, MJ. Recycled microbial mortar: Effects of bacterial concentration and calcium lactate content. Construction and Building Materials. 2020;234:1-11. https://doi.org/10.1016/j.conbuildmat.2019.117349
[27] Zhang Y, Pan Y, Ren T, Liang H, Zhang J, Zhang D. The Application of Calcium-Based Expansive Agents in High-Strength Concrete: A Review. Buildings. 2024;14(8):2369. https://doi.org/10.3390/buildings14082369
[28] Stanaszek-Tomal E. Bacterial concrete as a sustainable building material? Sustainability. 2020;12(2):696. https://doi.org/10.3390/su12020696
[29] Zhang Y, Guo HX, Cheng XH. Role of calcium sources in the strength and microstructure of microbial mortar. Construction and Building Materials. 2015;77:160-7. https://doi.org/10.1016/j.conbuildmat.2014.12.040
[30] Erşan YÇ, Verbruggen H, De Graeve I, Verstraete W, De Belie N, Boon N. Nitrate reducing CaCO3 precipitating bacteria survive in mortar and inhibit steel corrosion. Cement and Concrete Research. 2016;83:19-30. https://doi.org/10.1016/j.cemconres.2016.01.009
[31] Erşan YÇ, Belie Nd, Boon N. Microbially induced CaCO3 precipitation through denitrification: An optimization study in minimal nutrient environment. Biochemical Engineering Journal. 2015;101:108-18. https://doi.org/10.1016/j.bej.2015.05.006
[32] Heikal M. Effect of calcium formate as an accelerator on the physicochemical and mechanical properties of pozzolanic cement pastes. Cement and Concrete Research. 2004;34(6):1051-6. https://doi.org/10.1016/j.cemconres.2003.11.015
[33]Tziviloglou E, Van Tittelboom K, Palin D, Wang J, Sierra-Beltrán MG, Erşan YÇ, et al. Bio-Based Self-Healing Concrete: From Research to Field Application. 2016;273:345-85. https://doi.org/10.1007/12_2015_332
[34] Mors R, Jonkers H. Feasibility of lactate derivative based agent as additive for concrete for regain of crack water tightness by bacterial metabolism. Industrial crops and products. 2017;106:97-104. https://doi.org/10.1016/j.indcrop.2016.10.037
[35] Perrin A, Gagné R, Tran N, Petit L, Lors C. Large-scale apparatus for the quantitative evaluation of biorepair in a cracked concrete slab. Construction and Building Materials. 2024;448:138174. https://doi.org/10.1016/j.conbuildmat.2024.138174
[36] Chaerun SK, Syarif R, Wattimena RK. Bacteria incorporated with calcium lactate pentahydrate to improve the mortar properties and self-healing occurrence. Scientific reports. 2020;10(1):17873. https://doi.org/10.1038/s41598-020-74127-4
[37] Mokhtar N, Johari MAM, Tajarudin HA, Al-Gheethi AA, Algaifi HA. A sustainable enhancement of bio-cement using immobilised Bacillus sphaericus: Optimization, microstructural properties, and techno-economic analysis for a cleaner production of bio-cementitious mortars. Journal of Cleaner Production. 2021;318:128470. https://doi.org/10.1016/j.jclepro.2021.128470

[38] Ann KY, Jung HS, Kim HS, Kim SS, Moon HY. Effect of calcium nitrite-based corrosion inhibitor in preventing corrosion of embedded steel in concrete. Cement and Concrete Research. 2006;36(3):530-5. https://doi.org/10.1016/j.cemconres.2005.09.003
[39] Bandlamudi RK, Dutta JR, Kar A. Applications of microbial calcium carbonate precipitation in concrete through denitrification: a review. Innovative Infrastructure Solutions. 2023;8(4):113. https://doi.org/10.1007/s41062-023-01075-z
[40] Omoregie AI, Wong CS, Rajasekar A, Ling JH, Laiche AB, Basri HF, et al. Bio-Based Solutions for Concrete Infrastructure: A Review of Microbial-Induced Carbonate Precipitation in Crack Healing. Buildings. 2025;15(7):1052. https://doi.org/10.3390/buildings15071052
[41] Tao H, Jiang P, Qu J, Huang Y. The impact of various calcium ion sources on the curing efficacy of MICP. Scientific Reports. 2025;15(1):9149. https://doi.org/10.1038/s41598-025-94124-9
[42] El Enshasy H, Dailin DJ, Malek RA, Nordin NZ, Keat HC, Eyahmalay J, et al. Biocement: A Novel Approach in the Restoration of Construction Materials. In: Yadav AN, Rastegari AA, Gupta VK, Yadav N, editors. Microbial Biotechnology Approaches to Monuments of Cultural Heritage. Singapore: Springer; 2020. p. 177-98. https://doi.org/10.1007/978-981-15-3401-0_10
[43] Ali M, Mukhtar H, Dufossé L. Microbial calcite induction: a magic that fortifies and heals concrete. International Journal of Environmental Science and Technology. 2023;20(1):1113-34. https://doi.org/10.1007/s13762-022-03941-2
[44] Wang Y, Wang Y, Konstantinou C. Strength behavior of temperature-dependent MICP-treated soil. Journal of Geotechnical and Geoenvironmental Engineering. 2023;149(12):04023116. https://doi.org/10.1061/JGGEFK.GTENG-11526
[45] Algaifi HA, Bakar SA, Sam ARM, Ismail M, Abidin ARZ, Shahir S, et al. Insight into the role of microbial calcium carbonate and the factors involved in self-healing concrete. Construction and building materials. 2020;254:119258. https://doi.org/10.1016/j.conbuildmat.2020.119258
[46] Seifan M, Berenjian A. Microbially induced calcium carbonate precipitation: a widespread phenomenon in the biological world. Applied Microbiology and Biotechnology. 2019;103(12):4693-708. https://doi.org/10.1007/s00253-019-09861-5
[47] Chen H-J, Peng C-F, Tang C-W, Chen Y-T. Self-Healing Concrete by Biological Substrate. Materials. 2019;12(24). https://doi.org/10.3390/ma12244099
[48] Seifan M. Self-healing concrete: a novel nanobiotechnological approach to heal the concrete cracks: The University of Waikato; 2018.
[49] Justo-Reinoso I, Heath A, Gebhard S, Paine K. Aerobic non-ureolytic bacteria-based self-healing cementitious composites: A comprehensive review. Journal of Building Engineering. 2021;42:102834. https://doi.org/10.1016/j.jobe.2021.102834
[50] Wani S, Gęca MJ, Selvaraj T, Priya TS. Assessing the influence of Bacillus megaterium and Bacillus sphaericus in cementitious materials: Promoting sustainability towards strength, durability and crack repair. Ain Shams Engineering Journal. 2024;15(6):102748. https://doi.org/10.1016/j.asej.2024.102748
[51] Paine K, Alazhari M, Sharma T, Cooper R, Heath A, editors. Design and performance of bacteria-based self-healing concrete. The 9th International Concrete Conference 2016: Environment, Efficiency and Economic Challenges for Concrete; 2016.
[52] Luo M, Qian C. Influences of bacteria-based self-healing agents on cementitious materials hydration kinetics and compressive strength. Construction and Building Materials. 2016;121:659-63. https://doi.org/10.1016/j.conbuildmat.2016.06.075
[53] Coico R. Current protocols in microbiology: Wiley; 2006. https://doi.org/10.1002/9780471729259
[54] Sneath PH, Mair NS, Sharpe ME, Holt JG. Bergey's manual of systematic bacteriology. Volume 21986.
[55] Shruthi V, Tangadagi RB, Shwetha K, Nagendra R, Ranganath C, Ganesh B. Strength and drying shrinkage of high strength self-consolidating concrete. Recent Trends in Civil Engineering: Select Proceedings of ICRTICE 2019; 2021: Springer. https://doi.org/10.1007/978-981-15-5195-6_48
[56] Sk A, Rohit M, Sachin M, Babu R. Self-Healing Concrete Using Bacteria. 2020.
[57] Biswal US, Mishra M, Singh MK, Pasla D. Experimental investigation and comparative machine learning prediction of the compressive strength of recycled aggregate concrete incorporated with fly ash, GGBS, and metakaolin. Innovative Infrastructure Solutions. 2022;7(4):242. https://doi.org/10.1007/s41062-022-00844-6
[58] Kumar M, Kumar A, Solanki D, Mungule M. Low molarity geopolymer concrete: Effects on compressive strength, elastic modulus, sorptivity and chloride migration. Construction and Building Materials. 2023;409:134065. https://doi.org/10.1016/j.conbuildmat.2023.134065
[59] Neethu S, Tensing D, Vincent Sam Jebadurai S, Vincent S. Effect of sea sand in the behaviour of fresh concrete partially replaced with M-sand. Research on Engineering Structures and Materials. 2024;10(1):91-110.
[60] Vijay K, Murmu M, Deo SV. Bacteria based self- healing concrete - A review. Construction and Building Materials. 2017;152:1008-14. https://doi.org/10.1016/j.conbuildmat.2017.07.040

[61] Malathy R, Subramanian K. Drying shrinkage of cementitious composites with mineral admixtures. 2007.
[62] Joshi S, Goyal S, Mukherjee A, Reddy MS. Protection of concrete structures under sulfate environments by using calcifying bacteria. Construction and Building Materials. 2019;209:156-66. https://doi.org/10.1016/j.conbuildmat.2019.03.079
[63] Pitroda J. Assessment of sorptivity and water absorption of concrete with partial replacement of cement by fly ash and hypo sludge. IJARESM. 2015;1(2):33-42.
[64] Wiktor V, Jonkers HM. Quantification of crack-healing in novel bacteria-based self-healing concrete. Cement and Concrete Composites. 2011;33(7):763-70. https://doi.org/10.1016/j.cemconcomp.2011.03.012
[65] Wani S, Jan Gęca M, Selvaraj T, Shanmuga Priya T. Assessing the influence of Bacillus megaterium and Bacillus sphaericus in cementitious materials: Promoting sustainability towards strength, durability and crack repair. Ain Shams Engineering Journal. 2024;15(6):102748. https://doi.org/10.1016/j.asej.2024.102748
[66] Wang J, Soens H, Verstraete W, De Belie N. Self-healing concrete by use of microencapsulated bacterial spores. Cement and concrete research. 2014;56:139-52. https://doi.org/10.1016/j.cemconres.2013.11.009
[67] Van Tittelboom K, De Belie N, De Muynck W, Verstraete W. Use of bacteria to repair cracks in concrete. Cement and concrete research. 2010;40(1):157-66. https://doi.org/10.1016/j.cemconres.2009.08.025
[68] Stocks-Fischer S, Galinat JK, Bang SS. Microbiological precipitation of CaCO3. Soil Biology and Biochemistry. 1999;31(11):1563-71. https://doi.org/10.1016/S0038-0717(99)00082-6
[69] Das AK, Mallik M, Kalita P, Tag H. Optimization of Biogenic Calcium Carbonate Production Using Bamboo Dust as a Nutrient Source by Bacillus subtilis and Bacillus cereus for Enhanced Self-Healing Concrete. Journal of the Indian Chemical Society. 2025:101715. https://doi.org/10.1016/j.jics.2025.101715
[70] Nguyen MT, Fernandez CA, Haider MM, Chu KH, Jian G, Nassiri S, et al. Toward Self-Healing Concrete Infrastructure: Review of Experiments and Simulations across Scales. Chem Rev. 2023;123(18):10838-76. https://doi.org/10.1021/acs.chemrev.2c00709
[71] Shashank BS, Kumar.K P, Nagaraja PS. Fracture behavior study of self-healing bacterial concrete. Materials Today: Proceedings. 2022;60:267-74. https://doi.org/10.1016/j.matpr.2021.12.520
[72] Gat D, Tsesarsky M, Shamir D. Ureolytic calcium carbonate precipitation in the presence of non-ureolytic competing bacteria. Geo-Frontiers 2011: Advances in Geotechnical Engineering2011. p. 3966-74. https://doi.org/10.1061/41165(397)405
[73] Meng Q, Wang D, Fu X, Geng W, Zheng H, Bai W. Converting Bacillus subtilis 168 to a Synthetic Methylotroph by Combinatorial Metabolic Regulation Strategies. Journal of Agricultural and Food Chemistry. 2025. https://doi.org/10.1021/acs.jafc.4c09781
[74] Das AK, Mallik M, Kalita P, Tag H. Optimization of biogenic calcium carbonate production using bamboo dust as a nutrient source by Bacillus subtilis and Bacillus cereus for enhanced self-healing concrete. Journal of the Indian Chemical Society. 2025;102(6):101715. https://doi.org/10.1016/j.jics.2025.101715
[75] Qian S, Li J, Xu T, Diao E, Tang Y, Zhou X, et al. Calcium lactate efficiently induces production of bacillomycin D in Bacillus subtilis NS-174 and inhibition of spore germination of Aspergillus flavus in rice. International Journal of Food Science and Technology. 2023;58(2):824-30. https://doi.org/10.1111/ijfs.16241
[76] Hungria R, Mousa M, Hassan MM, Arce G, Omar O, Gavilanes A, et al. Self-Healing Efficiency of Cementitous Mortar Using Different Bacteria Protection Methods and Mineral Precursors. Journal of Materials in Civil Engineering. 2024;36(1):04023520. https://doi.org/10.1061/JMCEE7.MTENG-16130
[77] Zhu T, Dittrich M. Carbonate precipitation through microbial activities in natural environment, and their potential in biotechnology: a review. Frontiers in bioengineering and biotechnology. 2016;4:4. https://doi.org/10.3389/fbioe.2016.00004
[78] Liu J, Yu C, Shu X, Ran Q, Yang Y. Recent advance of chemical admixtures in concrete. Cement and Concrete Research. 2019;124:105834. https://doi.org/10.1016/j.cemconres.2019.105834
[79] Vaezi M, Zareei SA, Jahadi M. Recycled microbial mortar: Effects of bacterial concentration and calcium lactate content. Construction and Building Materials. 2020;234:117349. https://doi.org/10.1016/j.conbuildmat.2019.117349
[80] Irwan J, Anneza L, Othman N, Faisal Alshalif A. Compressive strength and water penetration of Concrete with Enterococcus Faecalis and calcium lactate. Key Engineering Materials. 2016;705:345-9. https://doi.org/10.4028/www.scientific.net/KEM.705.345
[81] Vijay K, Murmu M. Effect of calcium lactate on compressive strength and self-healing of cracks in microbial concrete. Frontiers of Structural and Civil Engineering. 2019;13:515-25. https://doi.org/10.1007/s11709-018-0494-2
[82] Ammar MA, Chegenizadeh A, Budihardjo MA, Nikraz H. The Effects of Crystalline Admixtures on Concrete Permeability and Compressive Strength: A Review. Buildings. 2024;14(9):3000. https://doi.org/10.3390/buildings14093000

[83] Erşan Y, Akin Y. Optimizing nutrient content of microbial self-healing concrete. 2018.
[84] Kardogan B, Sekercioglu K, Erşan YÇ. Compatibility and biomineralization oriented optimization of nutrient content in nitrate-reducing-biogranules-based microbial self-healing concrete. Sustainability. 2021;13(16):8990. https://doi.org/10.3390/su13168990
[85] Dong J, Wu H, Xie S, Shang X, Shi Z, Tu Z, et al. Impact of calcium formate and anhydrous sodium sulfate on the flowability, mechanical properties, and hydration characteristics of UHPC. Journal of Building Engineering. 2024;96:110534. https://doi.org/10.1016/j.jobe.2024.110534
[86] Chen L, Jiang L, Liu X, Xu P, Meng Y, Ben X, et al. Understanding the role of calcium formate towards hydration and deformation property of light-burned magnesia cement. Construction and Building Materials. 2021;289:122995. https://doi.org/10.1016/j.conbuildmat.2021.122995
[87] Abo Sabah SH, Anneza LH, Juki MI, Alabduljabbar H, Othman N, Al-Gheethi AA, et al. The Use of Calcium Lactate to Enhance the Durability and Engineering Properties of Bioconcrete. Sustainability. 2021;13(16):9269. https://doi.org/10.3390/su13169269
[88] Zanjad N, Pawar S, Nayak C. Experimental study on different properties of cenosphere based concrete using calcium lactate. Sigma Journal of Engineering and Natural Sciences. 2024;42(6):1786-96. https://doi.org/10.14744/sigma.2023.00132
[89] Irwan J, Anneza L, Othman N, Alshalif AF, Zamer M, Teddy T, editors. Calcium Lactate addition in Bioconcrete: Effect on Compressive strength and Water penetration. MATEC Web of Conferences; 2016: EDP Sciences. https://doi.org/10.1051/matecconf/20167801027
[90] Ducasse-Lapeyrusse J, Gagné R, Lors C, Damidot D. Effect of calcium gluconate, calcium lactate, and urea on the kinetics of self-healing in mortars. Construction and Building Materials. 2017;157:489-97. https://doi.org/10.1016/j.conbuildmat.2017.09.115
[91] Irwan JM, Anneza LH, Othman N, Alshalif AF, Zamer MM, Teddy T. Mechanical Properties of Concrete with Enterococcus Faecalis and Calcium Lactate. Procedia Engineering. 2017;171:592-7. https://doi.org/10.1016/j.proeng.2017.01.381
[92] Rusu MM, Faux D, Ardelean I. Monitoring the Effect of Calcium Nitrate on the Induction Period of Cement Hydration via Low-Field NMR Relaxometry. Molecules. 2023;28(2):476. https://doi.org/10.3390/molecules28020476
[93] Skripkiūnas G, Kičaitė A, Justnes H, Pundienė I. Effect of Calcium Nitrate on the Properties of Portland-Limestone Cement-Based Concrete Cured at Low Temperature. Materials. 2021;14(7):1611. https://doi.org/10.3390/ma14071611
[94] Erşan YÇ, Hernandez-Sanabria E, Boon N, de Belie N. Enhanced crack closure performance of microbial mortar through nitrate reduction. Cement and Concrete Composites. 2016;70:159-70. https://doi.org/10.1016/j.cemconcomp.2016.04.001
[95] Mirshahmohammad M, Rahmani H, Maleki-Kakelar M, Bahari A. Effect of sustained service loads on the self-healing and corrosion of bacterial concretes. Construction and Building Materials. 2022;322:126423. https://doi.org/10.1016/j.conbuildmat.2022.126423
[96] Bashaveni B, Pannem RMR. Case Studies in Construction Materials.
[97] Karagöl F, Demirboğa R, Kaygusuz MA, Yadollahi MM, Polat R. The influence of calcium nitrate as antifreeze admixture on the compressive strength of concrete exposed to low temperatures. Cold Regions Science and Technology. 2013;89:30-5. https://doi.org/10.1016/j.coldregions.2013.02.001
[98] Khan MNN, Kuri JC, Sarker PK. Effect of waste glass powder as a partial precursor in ambient cured alkali activated fly ash and fly ash-GGBFS mortars. Journal of Building Engineering. 2021;34:101934. https://doi.org/10.1016/j.jobe.2020.101934
[99] Muhammad S, Siddiqui HA, Abro MI, Usmani A, Mallick MAA. Bacillus subtilis as self-healing agent in cement mortar: Combined and the separate effect of bacteria and calcium lactate on self-healing behavior in cement mortar. Mehran University Research Journal Of Engineering & Technology. 2021;40(2):426-34. https://doi.org/10.22581/muet1982.2102.16
[100] Mammoliti L. Examination of the mechanism of corrosion inhibition by calcium nitrite and calcium nitrate-based admixtures in concrete. 2001.
[101] Huseien GF, Memon RP, Baghban MH, Faridmehr I, Wong LS. Effective microorganism solution-imbued sustainable self-curing concrete: Evaluation of sorptivity, drying shrinkage and expansion. Case Studies in Construction Materials. 2024;20:e03255. https://doi.org/10.1016/j.cscm.2024.e03255
[102] Pappupreethi K, Ammakunnoth R, Magudeaswaran P. Bacterial concrete: A review. International Journal of Civil Engineering and Technology. 2017;8(2):588-94.
[103] Mors R, Jonkers H. Effect on concrete surface water absorption upon addition of lactate derived agent. Coatings. 2017;7(4):51. https://doi.org/10.3390/coatings7040051
[104] De Belie N, Wang J, Bundur ZB, Paine K. Bacteria-based concrete. Eco-efficient repair and rehabilitation of concrete infrastructures: Elsevier; 2018. p. 531-67. https://doi.org/10.1016/B978-0-08-102181-1.00019-8

[105] Abo-El-Enein S, Ali A, Talkhan FN, Abdel-Gawwad H. Application of microbial biocementation to improve the physico-mechanical properties of cement mortar. Hbrc Journal. 2013;9(1):36-40. https://doi.org/10.1016/j.hbrcj.2012.10.004
[106] Luo M, Qian C-x, Li R-y. Factors affecting crack repairing capacity of bacteria-based self-healing concrete. Construction and Building Materials. 2015;87:1-7. https://doi.org/10.1016/j.conbuildmat.2015.03.117
[107] Luhar S, Luhar I, Shaikh FUA. A review on the performance evaluation of autonomous self-healing bacterial concrete: mechanisms, strength, durability, and microstructural properties. Journal of Composites Science. 2022;6(1):23. https://doi.org/10.3390/jcs6010023
[108] Feng J, Chen B, Sun W, Wang Y. Microbial induced calcium carbonate precipitation study using Bacillus subtilis with application to self-healing concrete preparation and characterization. Construction and Building Materials. 2021;280:122460. https://doi.org/10.1016/j.conbuildmat.2021.122460
[109] Vijay K, Murmu M. Experimental Study on Bacterial Concrete Using Bacillus Subtilis Micro-Organism. Emerging Trends in Civil Engineering: Springer; 2020. p. 245-52. https://doi.org/10.1007/978-981-15-1404-3_20
[110] Osman KM, Taher FM, Abd El-Tawab A, Faried AS. Role of different microorganisms on the mechanical characteristics, self-healing efficiency, and corrosion protection of concrete under different curing conditions. Journal of Building Engineering. 2021;41:102414. https://doi.org/10.1016/j.jobe.2021.102414
[111] Erşan YÇ, Da Silva FB, Boon N, Verstraete W, De Belie N. Screening of bacteria and concrete compatible protection materials. Construction and Building Materials. 2015;88:196-203. https://doi.org/10.1016/j.conbuildmat.2015.04.027
[112] Kanellopoulos A, Qureshi T, Al-Tabbaa A. Glass encapsulated minerals for self-healing in cement based composites. Construction and Building Materials. 2015;98:780-91. https://doi.org/10.1016/j.conbuildmat.2015.08.127
[113] De Muynck W, Debrouwer D, De Belie N, Verstraete W. Bacterial carbonate precipitation improves the durability of cementitious materials. Cement and Concrete Research. 2008;38(7):1005-14. https://doi.org/10.1016/j.cemconres.2008.03.005
[114] Chahal N, Siddique R, Rajor A. Influence of bacteria on the compressive strength, water absorption and rapid chloride permeability of concrete incorporating silica fume. Construction and Building Materials. 2012;37:645-51. https://doi.org/10.1016/j.conbuildmat.2012.07.029
[115] Joshi S, Goyal S, Mukherjee A, Reddy MS. Microbial healing of cracks in concrete: a review. Journal of Industrial Microbiology and Biotechnology. 2017;44(11):1511-25. https://doi.org/10.1007/s10295-017-1978-0
[116] Khan MBE, Shen L, Dias-da-Costa D. Self-healing behaviour of bio-concrete in submerged and tidal marine environments. Construction and Building Materials. 2021;277:122332. https://doi.org/10.1016/j.conbuildmat.2021.122332
[117] Mitra A, Sreedharan SM, Singh R. Concrete Crack Restoration Using Bacterially Induced Calcium Metabolism. Indian Journal of Microbiology. 2021;61(2):229-33. https://doi.org/10.1007/s12088-020-00916-0
[118] De Souza Oliveira A, Toledo Filho RD, Fairbairn EdMR, de Oliveira LFC, Gomes OdFM. Microstructural characterization of self-healing products in cementitious systems containing crystalline admixture in the short-and long-term. Cement and Concrete Composites. 2022;126:104369. https://doi.org/10.1016/j.cemconcomp.2021.104369
[119] Harrington EA. X-ray diffraction measurements on some of the pure compounds concerned in the study of Portland cement. American journal of science. 1927;13(78):467-79. https://doi.org/10.2475/ajs.s5-13.78.467
[120] Chen H, Qian C, Huang H. Self-healing cementitious materials based on bacteria and nutrients immobilized respectively. Construction and Building Materials. 2016;126:297-303. https://doi.org/10.1016/j.conbuildmat.2016.09.023
[121] Jiang L, Jia G, Jiang C, Li Z. Sugar-coated expanded perlite as a bacterial carrier for crack-healing concrete applications. Construction and Building Materials. 2020;232:117-222. https://doi.org/10.1016/j.conbuildmat.2019.117222
[122] Kadapure SA, Deshannavar UB, Katageri BG, Kadapure PS. A systematic review on MICP technique for developing sustainability in concrete. European Journal of Environmental and Civil Engineering. 2023;27(16):4581-97. https://doi.org/10.1080/19648189.2023.2194942
[123] Maurente-Silva DG, Borowski JVB, Cappellesso VG, Vainstein MH, Masuero AB, Dal Molin DCC. Effect of Exposure Environment and Calcium Source on the Biologically Induced Self-Healing Phenomenon in a Cement-Based Material. Buildings. 2024;14(12):3782. https://doi.org/10.3390/buildings14123782

[124] Pinto A, González-Fonteboa B, Seara-Paz S, Martínez-Abella F. Effects of bacteria-based self-healing nutrients on hydration and rheology of cement pastes. Construction and Building Materials. 2023;404:133142. https://doi.org/10.1016/j.conbuildmat.2023.133142